Asai E. Wada T. Sakakibara Y. Toga A. Toma T. Shimizu T. Imai K. Nonoyama S. Morio T. Kamachi Y. Ohara O. Yachie A.	Analysis of mutations and recombination activity in RAG-deficient patient.	*Clin. Immunol.*	138	172-7	2011
Takagi M. Shinoda K. Piao J. Mitsuiki N. Takagi M. Matsuda K. Muramatsu H. Doisaki S. Nagasawa M.Morio T. Kasahara Y. Koike K. Kojima S. Takao A. MizutaniS.	Autoimmune Lymphoproliferative Syndrome Like Disease With Somatic KRAS Mutation.	*Blood.*	117	2887-90	2011
森尾友宏	分類不能型免疫不全症 Update	*Jpn.J.Clin.Immunol.*	35	14-22	2012
森尾友宏	分類不能型免疫不全症	炎症と免疫	19	17-22	2011
Nakagawa N, Imai K, Kanegane H, Sato H, Yamada M, Kondoh K, Okada S, Kobayashi M, Agematsu K, Takada H, Mitsuiki N, Oshima K, Ohara O, Suri D, Rawat A, Singh S, Pan-Hammarström Q, Hammarström L, Reichenbach J, Seger R, Ariga T, Hara T, Miyawaki T, Nonoyama S.	Quantification of kappa-deleting recombination excision 1 circles in Guthrie 2 cards for the identification of early B-cell maturation defects.	*J Allergy Clin Immunol,*	128	223-225	2011
Zhao M, Kanegane H, Kobayashi C, Nakazawa Y, Ishii E, Kasai M, Terui K, Gocho Y, Imai K, Kiyasu J, Nonoyama S, Miyawaki T.	Early and rapid detection of X-linked lymphoproliferative syndrome with SH2D1A mutations by flow cytometry.	*Cytometry B Clin Cytom.*	80	8-13	2011

Booth C, Gilmour KC, Veys P, Gennery AR, Slatter MA, Chapel H, Heath PT, Steward CG, Smith O, O'Meara A, Kerrigan H, Mahlaoui N, Cavazzana-Calvo M, Fischer A, Moshous D, Blanche S, Pachlopnik-Schmid J, Latour S, de Saint-Basile G, Albert M, Notheis G, Rieber N, Strahm B, Ritterbusch H, Lankester A, Hartwig NG, Meyts I, Plebani A, Soresina A, Finocchi A, Pignata C, Cirillo E, Bonanomi S, Peters C, Kalwak K, Pasic S, Sedlacek P, Jazbec J, Kanegane H, Nichols KE, Hanson IC, Kapoor N, Haddad E, Cowan M, Choo S, Smart J, Arkwright PD, Gaspar HB.	X-linked lymphoproliferative disease due to SAP/SH2D1A deficiency: a multicenter study on the manifestations, management, and outcome of the disease.	*Blood.*	117	53-62	2011
Pachlopnik Schmid J, Canioni D, Moshous D, Touzot F, Mahlaoui N, Hauck F, Kanegane H, Lopez Granados E, Mejstrikova E, Pellier I, Galicier L, Galambrun C, Barlogis V, Bordigoni P, Fourmaintraux A, Hamidou M, Dabadie A, Le Deist F, Haerynck F, Ouachée-Chardin M, Rohrlich P, Stephan JL, Lenoir C, Rigaud S, Lambert N, Milili	Clinical similarities and differences of patients with X-linked lymphoproliferative syndrome type 1 (XLP-1/SAP-deficiency) versus type 2 (XLP-2/XIAP-deficiency).	*Blood.*	117	1522-9	2011

M, Schiff C, Chapel H, Picard C, de Saint Basile G, Blanche S, Fischer A, Latour S.					
Yang X, Wang J, An YF, Kanegane H, Miyawaki T, Zhao XD.	Genetic and proteinic analysis of a Chinese boy with X-linked lymphoproliferative disease and his maternal relatives.	*Zhonghua Er Ke Za Zhi.*	49	416-20 (in Chinese)	2011
Yang X, Kanegane H, Nishida N, Imamura T, Hamamoto K, Miyashita R, Imai K, Nonoyama S, Sanayama K, Yamaide A, Kato K, Nagai K, Ishii E, van Zelm MC, Latour S, Zhao XD, Miyawaki T.	Clinical and genetic characteristics of XIAP deficiency in Japan.	*J Clin Immunol.*		Epub ahead of print	2012
金兼弘和、大坪慶輔、宮脇利男	制御性 T 細胞に異常を有する原発性免疫不全症	炎症と免疫	19	210-216	2011
金兼弘和	X 連鎖リンパ増殖症候群－SAP 欠損症と XIAP 欠損症	医学のあゆみ	238	1058-1064	2011
Kondo Y, Iizuka M, Wakamatsu E, Yao Z, Tahara M, Tsuboi H, Sugihara M, Hayashi T, Yoh K, Takahiashi S, Matsumoto I, Sumida T.	Overexpression of T-bet gene regulates murine autoimmune arthritis.	*Arthritis Rheum.*	64	162-72	2012
Nakagawa N, Imai K, Kanegane H, Sato H, Yamada M, Kondoh K, Okada S, Kobayashi M, Agematsu K, Takada H, Mitsuiki N, Oshima K, Ohara O, Suri D, Rawat A, Singh S, Pan-Hammarström Q, Hammarström L, Reichenbach J, Seger R, Ariga T, Hara T, Miyawaki T, Nonoyama S.	Quantification of κ-deleting recombination excision circles in Guthrie cards for the identification of early B-cell maturation defects.	*J Allergy Clin Immunol.*	128	223-5.e2	2011

Murata Y, Yasumi T, Shirakawa R, Izawa K, Sakai H, Abe J, Tanaka N, Kawai T, Oshima K, Saito M, Nishikomori R, Ohara O, Ishii E, Nakahata T, Horiuchi H, Heike T.	Rapid diagnosis of FHL3 by flow cytometric detection of intraplatelet Munc13-4protein.	*Blood.*	118	1225-30	2011

V　研究成果の刊行物・別刷

nature immunology

The kinase Btk negatively regulates the production of reactive oxygen species and stimulation-induced apoptosis in human neutrophils

Fumiko Honda[1], Hirotsugu Kano[2], Hirokazu Kanegane[3], Shigeaki Nonoyama[4], Eun-Sung Kim[5], Sang-Kyou Lee[5], Masatoshi Takagi[1], Shuki Mizutani[1] & Tomohiro Morio[1]

The function of the kinase Btk in neutrophil activation is largely unexplored. Here we found that Btk-deficient neutrophils had more production of reactive oxygen species (ROS) after engagement of Toll-like receptors (TLRs) or receptors for tumor-necrosis factor (TNF), which was associated with more apoptosis and was reversed by transduction of recombinant Btk. Btk-deficient neutrophils in the resting state showed hyperphosphorylation and activation of phosphatidylinositol-3-OH kinase (PI(3)K) and protein tyrosine kinases (PTKs) and were in a 'primed' state with plasma membrane–associated GTPase Rac2. In the absence of Btk, the adaptor Mal was associated with PI(3)K and PTKs at the plasma membrane, whereas in control resting neutrophils, Btk interacted with and confined Mal in the cytoplasm. Our data identify Btk as a critical gatekeeper of neutrophil responses.

Among 'professional' phagocytes with a sophisticated arsenal of microbicidal features, neutrophils are the dominant cells that mediate the earliest innate immune responses to microbes[1–3]. Neutrophils migrate to the site of infection, sense and engulf microorganisms, produce reactive oxygen species (ROS) and kill the invading microbes via ROS by acting together with antimicrobial proteins and peptides[1,2]. The enzyme responsible for the respiratory burst is NADPH oxidase, which catalyzes the production of superoxide from oxygen and NADPH. This enzyme is a multicomponent complex that consists of membrane-bound flavocytochrome b_{558} (gp91^{phox} and p22^{phox}), cytosolic components (p47^{phox}, p67^{phox} and p40^{phox}) and a GTPase (Rac1 or Rac2)[3–6]. Activation of NADPH oxidase is strictly regulated both temporally and spatially to ensure that the reaction takes place rapidly at the appropriate cellular localization. Activation of this system requires three signaling triggers, including protein kinases, lipid-metabolizing enzymes and nucleotide-exchange factors that activate the Rac GTPase[3–6].

Inadequate production of ROS is associated with various human pathological conditions. Deficiency of any component of the NADPH oxidase complex results in chronic granulomatous disease, in which bacterial and fungal infections are recurrent and life-threatening[4]. Abnormalities in the molecules involved in the signal-transduction pathway initiated by the recognition of pathogen-associated molecular patterns are accompanied by less production of ROS after exposure to specific stimuli and by susceptibility to bacterial infection. These abnormalities include deficiency in the kinase IRAK4, the adaptor MyD88 deficiency or the kinase NEMO (IKKγ)[7]. In contrast, many other human disorders are believed to be associated with or induced by excessive production of ROS that causes DNA damage, tissue damage, cellular apoptosis and neutropenia[8,9].

Here we focus on determining the role of the kinase Btk in production of ROS and cellular apoptosis in human neutrophils, as 11–30% of patients with X-linked agammaglobulinemia (XLA), a human disease of Btk deficiency, have neutropenia[10,11], and Btk is a critical signaling component of phagocytic cells[12–14]. The neutropenia of XLA is distinct from that of common variable immunodeficiency (CVID) in that the neutropenia is induced by infection, is usually ameliorated after supplementation with immunoglobulin and is not mediated by the autoimmune response[10,11,14]. Although a few reports have suggested that myeloid differentiation is impaired in mice with X-linked immunodeficiency[15,16], the reason for the infection-triggered neutropenia is unknown. The role of Btk in human neutrophils remains largely unexplored.

Btk is a member of the Tec-family kinases (TFKs) that are expressed in hematopoietic cells such as B cells, monocytes, macrophages and neutrophils[12]. It has a crucial role in cell survival, proliferation, differentiation and apoptosis, especially in cells of the B lineage. In humans with XLA, B cells fail to reach maturity and are presumably doomed to premature death by the *BTK* mutation that leads to the XLA phenotype[17]. Both mice with X-linked immunodeficiency that have natural mutations in *Btk* and mice in which *Btk* is targeted have B cell defects, but these are associated with much milder effects than those seen in XLA, which suggests species differences in the role of Btk[18,19].

[1]Department of Pediatrics and Developmental Biology, Tokyo Medical and Dental University Graduate School of Medical and Dental Sciences, Tokyo, Japan. [2]Department of Pediatrics, Teikyo University School of Medicine Hospital, Mizonokuchi, Kawasaki, Japan. [3]Department of Pediatrics, Toyama University School of Medicine, Toyama, Japan. [4]Department of Pediatrics, National Defense Medical College, Tokorozawa, Japan. [5]Department of Biotechnology, College of Life Science and Biotechnology, Yonsei University, Seoul, Republic of Korea. Correspondence should be addressed to T.M. (tmorio.ped@tmd.ac.jp).

Received 28 November 2011; accepted 12 January 2012; published online 26 February 2012; doi:10.1038/ni.2234

Btk is also an important signaling component of the innate immune system in phagocytic cells. Btk is involved in signaling via Toll-like receptors (TLRs) such as TLR2, TLR4, TLR7, TLR8 and TLR9, and is associated with the TLR adaptors MyD88, Mal (TIRAP) and IRAK1 (refs. 12–14,20–22). Defective innate immune responses have been observed in monocytes, dendritic cells, neutrophils and mast cells from Btk-deficient mice[12,14]. Neutrophils from mice with X-linked immunodeficiency have poor production of ROS and nitric oxide[15].

The contribution of Btk to the human innate immune system is less obvious. Stimulation via TLR2, TLR4, TLR7-TLR8 or TLR3 results in impaired production of tumor-necrosis factor (TNF) by dendritic cells from patients with XLA, whereas the TLR4-induced production of TNF and interleukin 6 (IL-6) by monocytes from patients with XLA remains intact[23–25]. Neutrophils from control subjects and patients with XLA show no substantial differences in their phosphorylation of the mitogen-activated protein kinases p38, Jnk and Erk induced by engagement of TLR4 or TLR7-TLR8 or production of ROS induced by the same stimuli[26].

Here we evaluate the role of Btk in the production of ROS and cellular apoptosis in human neutrophils through the use of Btk-deficient neutrophils, a protein-delivery system based on a cell-permeable peptide, and specific kinase inhibitors. Unexpectedly, and in contrast to published observations of mice with X-linked immunodeficiency[15], the production of ROS was substantially augmented in the absence of Btk in neutrophils stimulated via TLRs, the TNF receptor or phorbol 12-myristate 13-acetate (PMA) but not in monocytes or in lymphoblastoid B cell lines transformed by Epstein-Barr virus. Excessive production of ROS was associated with neutrophil apoptosis, which was reversed by the transduction of wild-type Btk protein. Btk-deficient neutrophils showed activation of key signaling molecules involved in the activation of NADPH oxidase, and this was accompanied by targeting of Rac2 to the plasma membrane. Mal was confined to the cytoplasm in association with Btk but was translocated to plasma membrane and interacted with protein tyrosine kinases (PTKs) and phosphatidylinositol-3-OH kinase (PI(3)K) in the absence of Btk. Here we present our findings on the mechanism by which Btk regulates the priming of neutrophils and the amplitude of the neutrophil response.

RESULTS

Excessive production of ROS in Btk-deficient neutrophils

To investigate the production of ROS in the absence of Btk, we monitored ROS in neutrophils, monocytes and Epstein-Barr virus–transformed lymphoblastoid B cell lines obtained from patients with XLA, healthy controls and patients with CVID (disease control) by staining with dihydrorhodamine 123 (DHR123) and a luminol chemiluminescence assay. PMA-driven production of ROS in Btk-deficient neutrophils was three to four times greater than that in neutrophils from healthy controls or patients with CVID, and we observed augmented production of ROS with a suboptimal dose of PMA, whereas the baseline production of ROS was similar (**Fig. 1a–d**). Similarly, and in contrast to published reports[26], engagement of TLR2 (with its ligand tripalmitoyl cysteinyl seryl tetralysine lipopeptide (Pam_3CSK_4)), TLR4 (with its ligand lipopolysaccharide) or the TNF receptor (with TNF) followed by stimulation with formyl-Met-Leu-Phe (fMLP), an agonist of G protein–coupled receptors, elicited augmented ROS responses in neutrophils from patients with XLA (**Fig. 1e,f**). The production of ROS was minimal after stimulation with the TLR9 agonist CpG-A in neutrophils from patients with XLA and was not significantly different from that of neutrophils from healthy controls. The observed phenomena were reproduced in Btk-deficient eosinophils but not in monocytes or Epstein-Barr virus–transformed lymphoblastoid B cell lines obtained from patients with XLA (**Supplementary Fig. 1**). These data indicated Btk-deficient neutrophils had excessive NADPH oxidase activity after various stimuli.

Augmented apoptosis in Btk-deficient neutrophils

Because high ROS concentrations are potentially harmful to cells, we investigated cell death induced by various stimuli in neutrophils from patients with XLA by staining with annexin V and the membrane-impermeable DNA-intercalating dye 7-AAD. Stimulation with PMA, TLR agonist plus fMLP, or TNF plus fMLP induced a significantly higher frequency of cells positive for annexin V among neutrophils from patients with XLA than among control neutrophils, whereas spontaneous cell death in the absence of stimulation was not significantly altered at 4 h in neutrophils from healthy controls versus those from patients with XLA (**Fig. 2a,b**). We observed cleavage of caspase-3, lower mitochondrial membrane potentials and degradation of proliferating

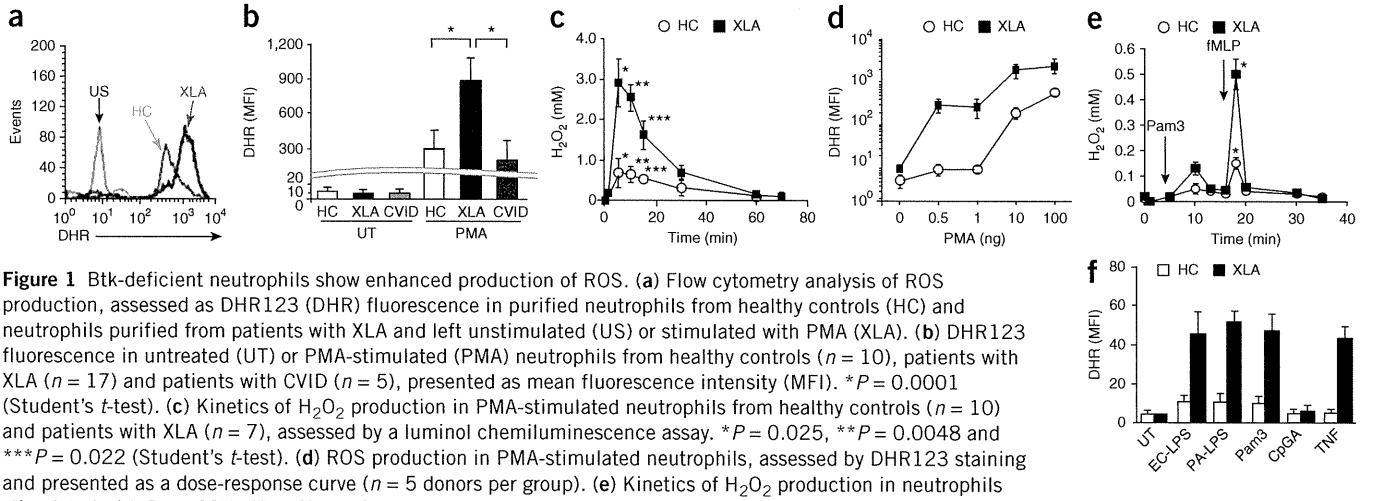

Figure 1 Btk-deficient neutrophils show enhanced production of ROS. (**a**) Flow cytometry analysis of ROS production, assessed as DHR123 (DHR) fluorescence in purified neutrophils from healthy controls (HC) and neutrophils purified from patients with XLA and left unstimulated (US) or stimulated with PMA (XLA). (**b**) DHR123 fluorescence in untreated (UT) or PMA-stimulated (PMA) neutrophils from healthy controls ($n = 10$), patients with XLA ($n = 17$) and patients with CVID ($n = 5$), presented as mean fluorescence intensity (MFI). $^*P = 0.0001$ (Student's t-test). (**c**) Kinetics of H_2O_2 production in PMA-stimulated neutrophils from healthy controls ($n = 10$) and patients with XLA ($n = 7$), assessed by a luminol chemiluminescence assay. $^*P = 0.025$, $^{**}P = 0.0048$ and $^{***}P = 0.022$ (Student's t-test). (**d**) ROS production in PMA-stimulated neutrophils, assessed by DHR123 staining and presented as a dose-response curve ($n = 5$ donors per group). (**e**) Kinetics of H_2O_2 production in neutrophils stimulated with Pam_3CSK_4 (Pam3) and fMLP, assessed by a luminol chemiluminescence assay ($n = 7$ donors per group). $^*P = 0.005$ (Student's t-test). (**f**) DHR123 fluorescence in neutrophils incubated with lipopolysaccharide from *Escherichia coli* (EC-LPS) or *Pseudomonas aeruginosa* (PA-LPS), Pam_3CSK_4, CpG-A or TNF, followed by stimulation with fMLP ($n = 7$ donors per group). Data are representative of seventeen experiments (**a**) or are pooled from at least five (**b**,**c**,**e**,**f**) or four (**d**) independent experiments (mean and s.d. in **b**–**f**).

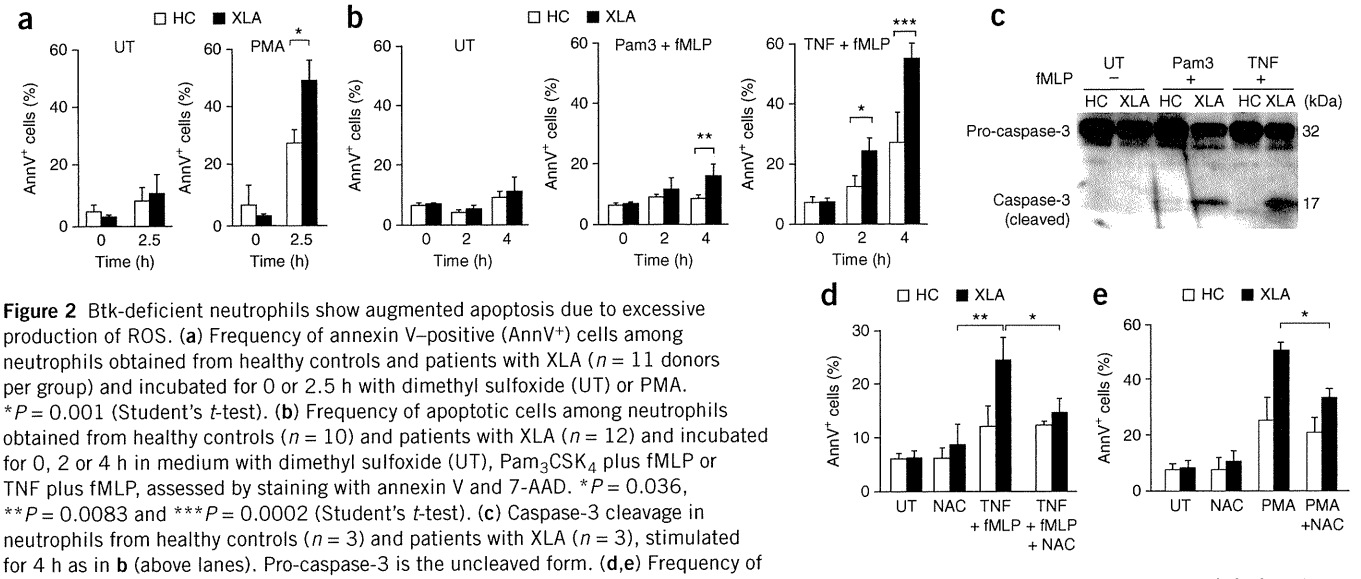

Figure 2 Btk-deficient neutrophils show augmented apoptosis due to excessive production of ROS. (**a**) Frequency of annexin V–positive ($AnnV^+$) cells among neutrophils obtained from healthy controls and patients with XLA ($n = 11$ donors per group) and incubated for 0 or 2.5 h with dimethyl sulfoxide (UT) or PMA. $^*P = 0.001$ (Student's *t*-test). (**b**) Frequency of apoptotic cells among neutrophils obtained from healthy controls ($n = 10$) and patients with XLA ($n = 12$) and incubated for 0, 2 or 4 h in medium with dimethyl sulfoxide (UT), Pam_3CSK_4 plus fMLP or TNF plus fMLP, assessed by staining with annexin V and 7-AAD. $^*P = 0.036$, $^{**}P = 0.0083$ and $^{***}P = 0.0002$ (Student's *t*-test). (**c**) Caspase-3 cleavage in neutrophils from healthy controls ($n = 3$) and patients with XLA ($n = 3$), stimulated for 4 h as in **b** (above lanes). Pro-caspase-3 is the uncleaved form. (**d**,**e**) Frequency of apoptotic Btk-deficient neutrophils ($n = 5$ donors) stimulated for 2 h (**d**) or 2.5 h (**e**) with the antioxidant N-acetyl-cysteine (NAC). $^*P = 0.043$ and $^{**}P = 0.036$ (**d**) or $^*P = 0.026$ (**e**; Student's *t*-test). Data are representative of three experiments (**b**) or at least five independent experiments (**a**,**c**–**e**; mean and s.d. in **a**,**b**,**d**,**e**).

cell nuclear antigen; hence, cell death was caused by apoptosis (**Fig. 2c** and **Supplementary Fig. 2**). Apoptosis assessed by these methods was augmented considerably for neutrophils from patients with XLA. The observed apoptosis was most probably triggered by ROS, as coincubation of neutrophils with N-acetyl cysteine, an antioxidant, rescued the cells from apoptosis induced by TNF plus fMLP or by PMA (**Fig. 2d,e**). We detected much more ROS release and stimulation-induced apoptosis of neutrophils from all patients with XLA regardless of the site or mode of their mutation (**Supplementary Fig. 3**). In addition, we found no correlation between genotype and the extent of neutrophil production of ROS. These data suggested that neutrophils from patients with XLA are susceptible to apoptosis triggered by pathogens.

Normalization of the ROS response by transduction of Btk

We next determined whether the enhanced apoptosis noted above was due to a defect in Btk itself or abnormal myeloid differentiation in the absence of Btk. For this, we prepared three recombinant Btk proteins (full-length Btk; Btk with deletion of the pleckstrin homology (PH) domain; and Btk with deletion of the kinase domain) fused to the cell-permeable peptide Hph-1 (**Fig. 3a,b**). We purified the products and transduced the proteins into neutrophils lacking Btk. The efficacy of transduction was more than 95%; and Hph-1–Btk expression was stable for at least 12–24 h (ref. 27). We adjusted the expression of Btk to that in neutrophils from healthy controls by incubating 1×10^6 cells for 1 h with 1 μM recombinant fusion protein. Transduction of full-length Btk into neutrophils from patients with XLA restored the production of ROS and the frequency of apoptotic cells after PMA stimulation to that observed for neutrophils from healthy controls (**Fig. 3c,d**). Transduction of the recombinant fusion of Btk with deletion of the PH domain only modestly reversed neutrophil overactivation (**Fig. 3c**), which indicated that appropriate cellular localization and interactions with other molecules were required for Btk function. Transduction of the recombinant fusion of Btk with deletion of the kinase domain minimally corrected excessive production of ROS (**Fig. 3c**), which suggested that the kinase activity of Btk or molecules that interacted via the kinase domain were critical for the regulation of ROS. We also confirmed the importance of the kinase domain by an experiment that showed excessive production of ROS in normal neutrophils treated with 50 μM LFM-A13, an inhibitor of the kinase activity of Btk, but not in those treated with LFM-A11, a control compound (**Fig. 3e**). We also documented augmented apoptosis in control neutrophils treated with LFM-A13 (**Fig. 3f**). These data demonstrated that the enhanced production of ROS and apoptosis was directly related to a defect in Btk.

NADPH oxidase components in Btk-deficient neutrophils

The NADPH oxidase complex consists of the transmembrane component ($gp91^{phox}$ and $p22^{phox}$), a cytosolic component ($p47^{phox}$, $p67^{phox}$ and $p40^{phox}$) and Rac2 (refs. 3–6). The activity of NADPH oxidase is controlled by targeting of the cytosolic components to the plasma membrane or phosphorylation of the cytosolic components or both. To assess the mechanism of the excessive production of ROS in Btk-deficient neutrophils, we investigated the abundance, phosphorylation and subcellular localization of each component by immunoblot analysis.

The expression of each component of the NADPH oxidase complex was similar in neutrophils from patients with XLA and those from healthy controls (**Fig. 4a**). The amount of $p47^{phox}$, $p67^{phox}$ and $p40^{phox}$ in the cytoplasm and the membrane was not substantially different in neutrophils from patients with XLA and those from healthy controls (**Fig. 4b**). Similarly, the amount in the membrane-targeted fraction after stimulation with PMA was not very different in neutrophils from patients with XLA and those from healthy controls (**Fig. 4c**). Phosphorylation of Ser345 in $p47^{phox}$ and of Thr154 in $p40^{phox}$ are important for translocation of the cytosolic components to the membrane[4,5,28]. Those modifications were not altered in Btk-deficient neutrophils (**Fig. 4c**). In contrast, we detected Rac2 in the plasma membrane of Btk-deficient neutrophils before stimulation with PMA. We observed four- to fivefold higher membrane expression of Rac2 in neutrophils from patients with XLA than in those from healthy controls in the resting state (**Fig. 4b**).

Typically, 10–15% of $gp91^{phox}$ is located in the plasma membrane of unstimulated neutrophils, whereas the majority of the molecule resides in specific granules. Membrane expression increases after

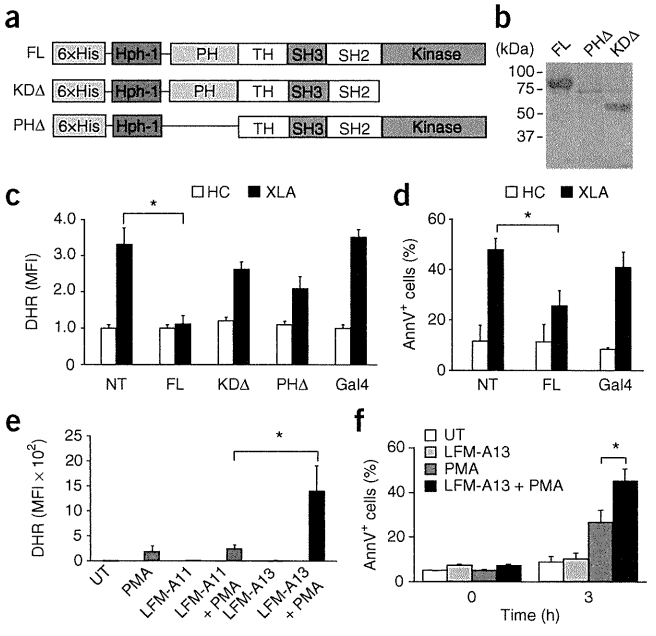

Figure 3 Excessive production of ROS and apoptosis in neutrophils from patients with XLA are abrogated by transduction of Hph-1–tagged full-length recombinant Btk but not by Hph-1–tagged Btk with deletion of the kinase or PH domain. (**a**) Hph-1–tagged Btk constructs: full-length Btk (FL); Btk with deletion of the kinase domain (KDΔ); Btk with deletion of the PH domain (PHΔ). 6×His, six-histidine tag; TH, Tec homology; SH3, Src homology 3; SH2, Src homology 2. (**b**) Size of purified Hph-1–tagged Btk proteins, confirmed by Coomassie brilliant blue staining. (**c**) ROS production in neutrophils from healthy controls ($n = 5$) and patients with XLA ($n = 5$), left untransduced (NT) or transduced with the constructs in **a** or Hph-1–tagged yeast transcriptional activator Gal4 (far right; control), presented as the MFI of DHR123 relative to that of untreated neutrophils from healthy controls, set as 1. (**d**) Frequency of apoptotic cells among neutrophils from healthy controls and patients with XLA, left untransduced or transduced with Hph-1–tagged full-length Btk or Gal4 (control). (**e**) DHR123 fluorescence in neutrophils from healthy controls ($n = 7$) left untreated or treated with PMA alone, or pretreated with LFM-A13 (Btk inhibitor) or LFM-A11 (control) alone or followed by stimulation with PMA (+ PMA). (**f**) Frequency of annexin V–positive cells among neutrophils from healthy controls ($n = 7$) left untreated or treated with PMA alone, or pretreated with LFM-A13 (50 μM, a concentration that does not inhibit other PTKs[47,48]) alone or followed by stimulation with PMA. $^*P = 0.0021$ (**c**), 0.019 (**d**), 0.021 (**e**) or 0.025 (**f**; Student's *t*-test). Data are representative of five experiments (**b**) or are pooled from six (**c**), three (**d**) or four (**e**,**f**) independent experiments (mean and s.d. in **c**–**f**).

signaling via TLRs or G protein–coupled receptors because of translocation to the plasma membrane[2]. Immunoblot analysis with antibody to gp91 (anti-gp91; **Fig. 4b**) and flow cytometry analysis of surface flavocytochrome b_{558} (**Fig. 4d**) showed higher gp91 expression in neutrophils from patients with XLA. Immunohistochemical analysis by confocal fluorescence microscopy showed localization of gp91 and Rac2 together in the membranes of resting Btk-deficient neutrophils but not in neutrophils from healthy controls (**Fig. 4e**). These results suggested that NADPH oxidase complex was partially assembled and ready to be activated in steady-state Btk-deficient neutrophils.

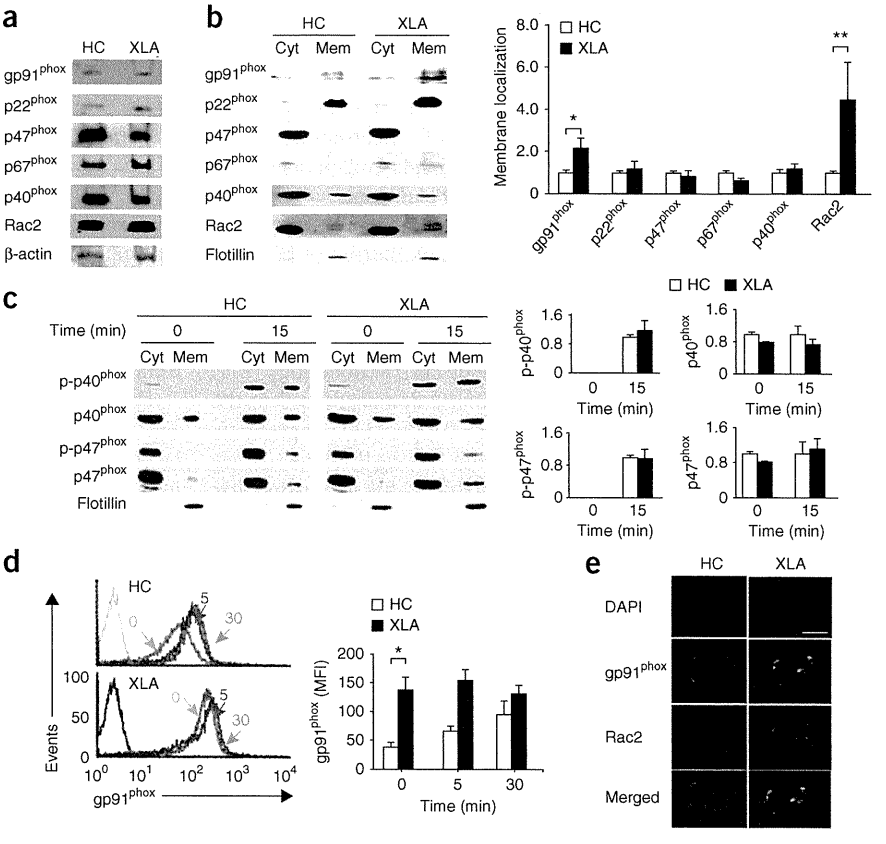

Figure 4 Btk-deficient neutrophils show targeting of Rac2 to the plasma membrane, colocalization of Rac2 with gp91^{phox} and higher membrane expression of gp91^{phox}. (**a**) Immunoblot analysis of the components of the NADPH oxidase complex in neutrophils from a healthy control and a patient with XLA. β-actin serves as a loading control throughout. (**b**) Immunoblot analysis (left) of the components of the NADPH oxidase complex in the cytoplasm (Cyt) and plasma membrane (Mem) of neutrophils from healthy controls and patients with XLA ($n = 9$ per group). Right, quantification of the membrane expression at left, presented as band intensity relative to that of flotillin (loading marker for the membrane-raft fraction) in membranes of neutrophils from healthy controls, set as 1. $^*P = 0.045$ and $^{**}P = 0.027$ (Student's *t*-test). (**c**) Immunoblot analysis of total and phosphorylated (p-) p40^{phox} and p47^{phox} in the cytoplasm and membrane of PMA-stimulated neutrophils from healthy controls and patients with XLA. Right, quantification as in **b**. (**d**) Flow cytometry analysis of gp91^{phox} on neutrophils from healthy controls and patients with XLA, left unstimulated (0) or stimulated for 5 or 30 min (above lines) with PMA, detected by staining with mAb 7D5 to gp91. Gray lines indicate staining with MsIgG (control). Right, quantification of the gp91 MFI in cells treated as at left. $^*P = 0.0039$ (Student's *t*-test). (**e**) Confocal microscopy of gp91^{phox} (green) and Rac2 (red) in healthy controls and neutrophils from patients with XLA; nuclei are counterstained with the DNA-intercalating dye DAPI (blue). Original magnification, ×600; scale bar, 10 μm. Data are from one representative of nine independent experiments with seven healthy controls and nine patients with XLA (**a**), are representative of nine experiments (**b**), are from nine independent experiments (**c**), are pooled from seven independent experiments (**d**) or are representative of four independent experiments (**e**; mean and s.d. in **b**–**d**).

Activated PTKs and PI(3)K in resting XLA neutrophils

Assembly and activation of the cytosolic components and Rac requires the involvement of kinases such as PTKs, PI(3)K and protein kinase C. We thus explored a potential signaling pathway that would lead to the partial assembly of NADPH oxidase. First, we examined the extent of tyrosine phosphorylation of cellular substrates in Btk-deficient and Btk-sufficient neutrophils before and after stimulation with PMA. Btk-deficient neutrophils showed hyperphosphorylation of protein species in the range of 50–53 kilodaltons (kDa), 72 kDa, 85 kDa and 150 kDa at baseline relative to phosphorylation in neutrophils from healthy controls (**Fig. 5a**). TLR4-mediated stimulation led to more phosphorylation of protein species 38 kDa, 50–53 kDa, 60 kDa, 72 kDa and 85 kDa in size in Btk-deficient neutrophils (**Supplementary Fig. 4a**).

In contrast, the baseline PTK activity in monocytes from patients with XLA was unaltered or slightly diminished relative to that of monocytes from healthy controls. TLR2-stimulated activation of PTKs was largely similar or slightly less in the absence of Btk (**Supplementary Fig. 4b**). We were able to directly ascribe the enhanced PTK activity to the absence of Btk, as transduction of recombinant Btk into neutrophils from patients with XLA restored baseline phosphorylation to that seen in neutrophils from healthy controls (**Fig. 5b**).

We next searched for tyrosine-phosphorylated proteins in Btk-deficient neutrophils through the use of phosphorylation-specific antibodies. The expression and activation of Tec and Bmx, TFKs present in neutrophils, was not upregulated in neutrophils from patients with XLA (**Fig. 5c**), which indicated that they did not compensate for Btk function. However, we found that the tyrosine-phosphorylated proteins 50–53 kDa, 72 kDa, 85 kDa and 150 kDa in size were the kinases Lyn and c-Src, Syk, the p85 subunit of PI(3)K (class IA) and FAK, respectively (**Fig. 5d,e**). We found that c-Src, Syk, PI(3)K-p85 and FAK were phosphorylated at their tyrosine residues that have a positive regulatory function. Notably, Lyn, a kinase known to have positive as well as negative roles in the modulation of myeloid function, was phosphorylated at Tyr507, a negative regulatory site[29–31].

We first focused on PI(3)K, as PI(3)K activation targets Rac2 to flavocytochrome b_{558}; this process is important for converting

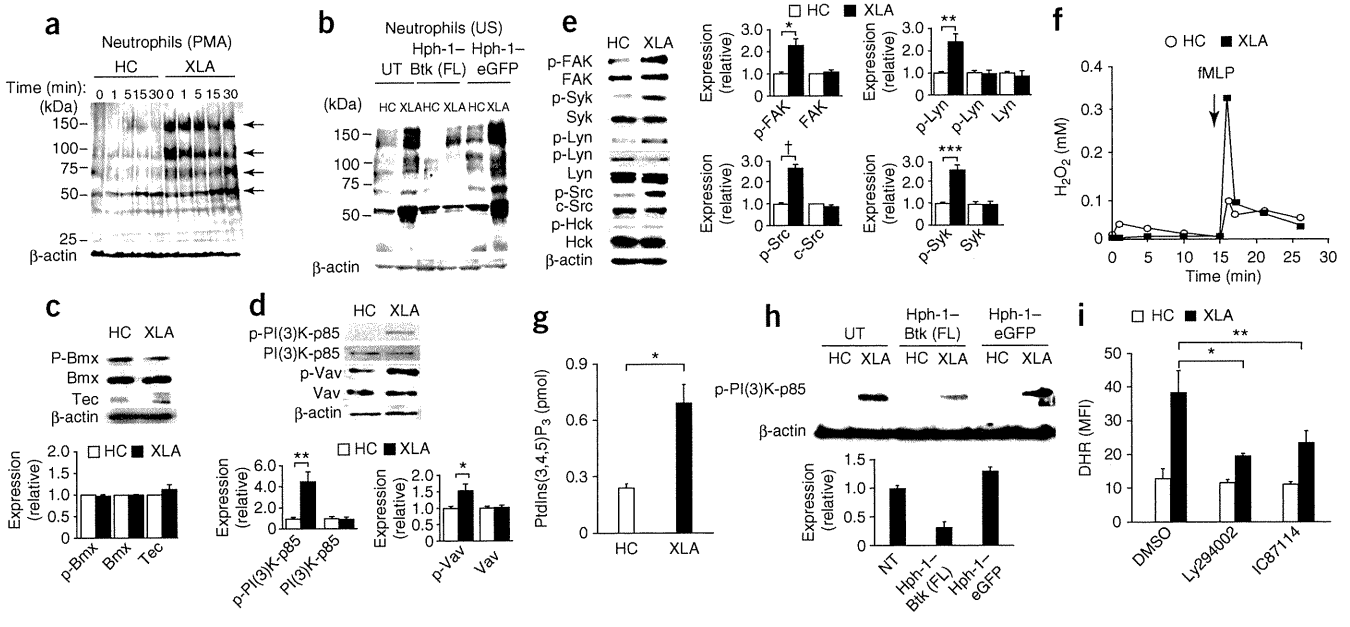

Figure 5 Btk-deficient neutrophils have higher baseline activity of PTKs and PI(3)K, which is reversed by transduction of recombinant Btk protein. (**a**) Immunoblot analysis of phosphorylated tyrosine in lysates of PMA-stimulated neutrophils from healthy controls ($n = 5$) and patients with XLA ($n = 7$). Arrows indicate hyperphosphorylated proteins in neutrophils from patients with XLA at 0 min. (**b**) Immunoblot analysis of phosphorylated tyrosine (as in **a**) in lysates from unstimulated (US) neutrophils from healthy controls ($n = 4$) and patients with XLA ($n = 5$), left untransduced or transduced with Hph-1-tagged full-length Btk or eGFP. (**c**,**d**) Immunoblot analysis (top) of whole-cell lysates of neutrophils from healthy controls ($n = 5$) and patients with XLA ($n = 7$), probed for total and phosphorylated Bmx and total Tec (**c**) or total and phosphorylated PI(3)K-p85 and Vav (phosphorylated at Tyr508 (PI(3)K-p85) or Tyr174 (Vav); **d**). Phosphorylated Tec was not detected by immunoblot analysis of phosphorylated tyrosine in samples immunoprecipitated with anti-Tec (data not shown). Bottom, quantification of the expression at top, presented relative to expression of β-actin in neutrophils from healthy controls, set as 1. $*P = 0.038$ and $**P = 0.0001$ (Student's *t*-test). (**e**) Immunoblot analysis (left) of neutrophils from healthy controls ($n = 5$) and patients with XLA ($n = 7$), probed for total PTKs and PTKs phosphorylated at Tyr576 and Tyr577 (FAK); Tyr524 and Tyr525 (Syk); Tyr507 (Lyn; top) or Tyr397 (Lyn; bottom); (Tyr416 (c-Src); and Tyr411 (the kinase Hck). Phosphorylated PTKs Fgr and Yes were undetectable (data not shown). Right, quantification as in **c**,**d**. $*P = 0.033$, $**P = 0.004$, $***P = 0.0007$ and $\dagger P = 0.0002$ (Student's *t*-test). (**f**) H_2O_2 production by fMLP-stimulated neutrophils from healthy controls and patients with XLA ($n = 5$ per group). (**g**) Enzyme-linked immunosorbent assay of phosphatidylinositol-(3,4,5)-trisphosphate (PtdIns(3,4,5)P_3) in unstimulated neutrophils from patients with XLA ($n = 5$). $*P = 0.0005$ (Student's *t*-test). (**h**) Immunoblot analysis (top) of phosphorylated PI(3)K-p85 in neutrophils from healthy controls and patients with XLA ($n = 5$ per group), left untransduced or transduced with Hph-1–tagged full-length Btk or eGFP. Detection of phosphorylated PI(3)K-p85 in neutrophils from healthy controls required longer exposure. Below, quantification of results above, presented relative to the expression of phosphorylated PI(3)K-p85 relative to that of β-actin in neutrophils from patients with XLA, set as 1. (**i**) Production of ROS in neutrophils from patients with XLA, treated with dimethyl sulfoxide (DMSO) or preincubated with Ly294002 (universal PI(3)K inhibitor; 50 μM)[32] or IC87114 (PI(3)Kδ inhibitor; 1 μM (a concentration that does not inhibit PI(3)Kα, PI(3)Kβ or PI(3)Kγ)[33]) and stimulated with fMLP. $*P = 0.006$ and $**P = 0.003$ (Student's *t*-test). Data are representative of or pooled from six (**a**,**f**), seven (**b**–**e**), four (**g**), eight (**h**) or five (**i**) independent experiments (mean and s.d. in **c**–**e**,**g**–**i**).

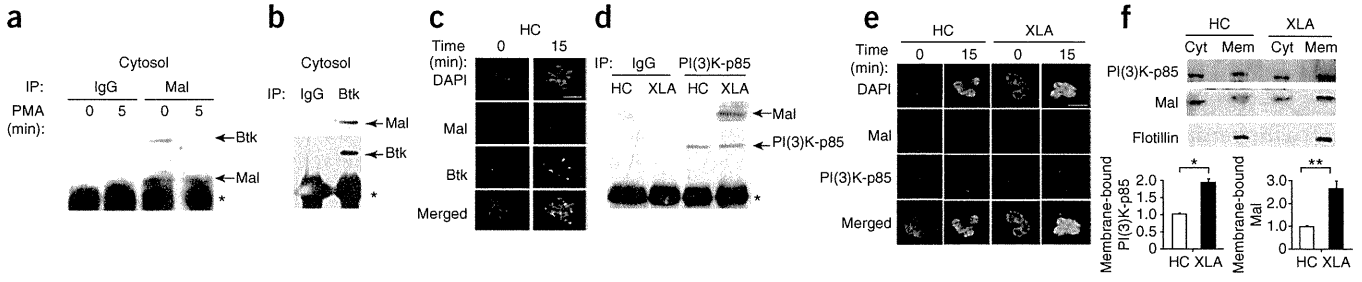

Figure 6 Mal in neutrophils from healthy controls associates with Btk in the resting state and translocates to the plasma membrane after stimulation, whereas Mal associates with PI(3)K at the plasma membrane in Btk-deficient neutrophils. (**a**,**b**) Coimmunoprecipitation analysis of Btk and Mal in the cytoplasmic fraction of neutrophils from healthy controls, left unstimulated (0 (**a**), **b**) or stimulated for 5 min with PMA (5 (**a**)). IP, immunoprecipitation; IgG, control antibody. *, immunoglobulin light chain (**a**) or heavy chain (**b**). (**c**) Confocal microscopy of neutrophils from healthy controls, left unstimulated (0) or stimulated for 15 min with PMA (15), then stained with anti-Mal (red) and anti-Btk (green) and counterstained with DAPI. Original magnification, ×600; scale bar, 10 μm. (**d**) Coprecipitation analysis of PI(3)K-p85 and Mal in membrane fraction of neutrophils from healthy controls and patients with XLA. *, immunoglobulin heavy chain. (**e**) Confocal microscopy of neutrophils from healthy controls and patients with XLA, left unstimulated or stimulated for 15 min with PMA, then stained with anti-Mal (red) and anti-PI(3)K-p85 (green) and counterstained with DAPI. Scale bar, 10 μm. (**f**) Immunoblot analysis (above) of PI(3)K-p85 and Mal in the cytoplasm and plasma membrane of unstimulated neutrophils from healthy controls and patients with XLA. Below, quantification of results above, presented relative to the expression of flotillin in neutrophils from healthy controls, set as 1. $*P = 0.0035$ and $**P = 0.0021$ (Student's *t*-test). Data are representative of three (**a**,**b**), four (**c**,**e**), six (**d**) or seven (**f**) independent experiments (mean and s.d. in **f**).

neutrophils into a 'primed' state in which they are ready for complete activation of NADPH oxidase triggered by stimuli such as fMLP. Indeed, Btk-deficient neutrophils were in a primed state, as fMLP alone elicited excessive production of ROS (**Fig. 5f**). Greater phosphorylation of PI(3)K-p85 was accompanied by more enzymatic activity, as shown by more baseline production of phosphatidylinositol-(3,4,5)-trisphosphate and by phosphorylation of the adaptor Vav (**Fig. 5d**,**g**). Furthermore, augmented PI(3)K activation was normalized, although only partially, by transduction of full-length Btk linked to Hph-1 (**Fig. 5h**).

The importance of PI(3)K in inducing the primed state was supported by data showing inhibition of fMLP-driven production of ROS by preincubation of Btk-deficient neutrophils with the universal PI(3)K inhibitor LY294002 at a concentration of 50 μM (refs. 32,33). We observed this inhibition in cells incubated with the PI(3)Kδ–specific inhibitor IC87114 at a concentration of 1 μM (ref. 33) but not in those incubated with the PI(3)Kγ–specific inhibitor AS605240 at a concentration of 8 nM (ref. 34; **Fig. 5i** and **Supplementary Fig. 5a**). These findings suggested PI(3)Kδ activation was involved in the excessive ROS response.

Interaction of membrane-targeted Mal with PI(3)K

We next sought the reason for the PI(3)K activation in the absence of Btk. For this, we first focused on a molecule that interacts with both Btk and PI(3)K. Evidence obtained with monocytes indicates that Mal is a critical component of TLR2-TLR4 signaling and is a target of Btk[13,14,20,21]. The TLR signal triggers activation of Btk, which in turn phosphorylates Mal. Phosphorylated Mal translocates to the plasma membrane via phosphatidylinositol-(4,5)-bisphosphate ($PtdIns(4,5)P_2$) and then interacts with and activates PI(3)K[35].

Unexpectedly, coimmunoprecipitation assays of neutrophils from human controls demonstrated that Mal was associated with Btk in the resting state (**Fig. 6a**,**b**). We observed colocalization of Mal and Btk in the cytoplasm and, after activation of cells with PMA, we detected the Mal-Btk complex at the membrane by immunofluorescence staining (**Fig. 6c**).

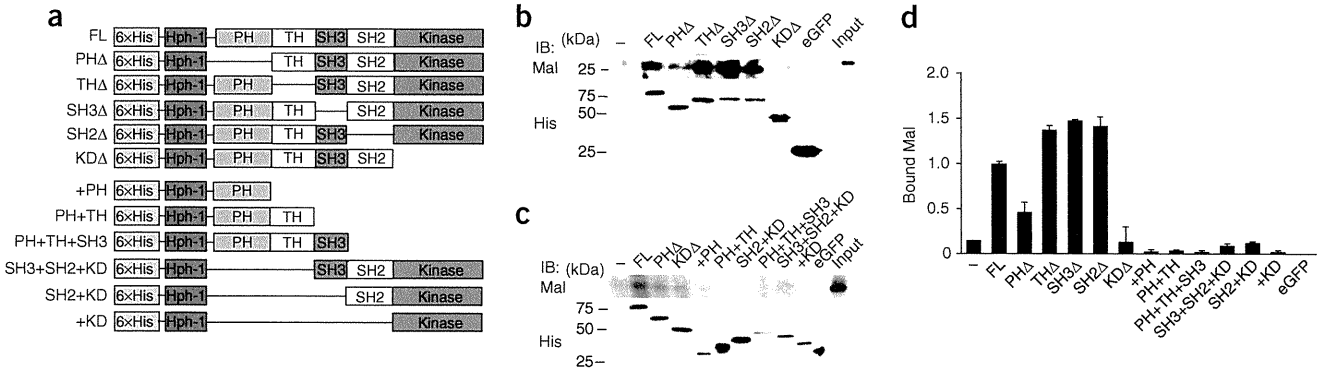

Figure 7 Btk associates with Mal at the PH and kinase domains. (**a**) Hph-1–tagged Btk constructs: full-length Btk (FL); Btk mutants with deletion of the PH domain (PHΔ), Tec homology (THΔ), SH3 domain (SH3Δ), SH2 domain (SH2Δ) or kinase domain (KDΔ); and Btk mutants with truncation retaining (+) only some domains (bottom six). (**b**,**c**) Immunoblot analysis (IB) of Mal (top) in extracts of cytoplasm of neutrophils from healthy controls, incubated with nickel beads bound to Hph-1–tagged recombinant full-length Btk or the deletion mutants (**b**) or truncation mutants (**c**) in **a**, or to Hph-1–tagged eGFP (negative control). Below, immunoblot analysis after rebinding to nickel beads, probed with anti-histidine (His). To make these as equimolar as possible, more beads were added for the +PH, PH+TH+SH3, SH3+SH2+KD and +KD constructs. Input, cytoplasmic extracts without precipitation. (**d**) Quantification of Mal bound to the recombinant Btk proteins based on the results in **b**,**c** ($n = 4$ donors), presented to results for full-length Btk, set as 1. Data are representative of four experiments (**b**,**c**) or are a summary of four independent experiments (**d**; mean and s.d.).

We did not detect the association of Mal with PI(3)K-p85 in unstimulated neutrophils from healthy controls; however, we did observe this association in Btk-deficient neutrophils before stimulation with PMA (**Fig. 6d**). Moreover, confocal fluorescence microscopy showed targeting of the PI(3)K-p85–Mal complex to the membrane in the absence of Btk, whereas we observed the complex at the membrane after stimulation with PMA in the presence of Btk (**Fig. 6e**). In addition, most of the PI(3)K-p85 and Mal was present in the membrane fraction in neutrophils from patients with XLA (**Fig. 6f**). These data suggested that Btk in resting neutrophils was involved in confining Mal to the cytoplasm.

The mode of the Btk-Mal association

Btk phosphorylates Mal at Tyr86, Tyr106 and Tyr187, and the Btk-Mal interaction requires Pro125, Tyr86, Tyr106 and Tyr159 in Mal, whereas the critical site in Btk for this association remains unknown[21,22]. To clarify the region of Btk required for the cytoplasmic Btk-Mal association, we generated various Btk deletion mutants fused to histidine-tagged Hph-1 (**Fig. 7a**) and assessed their binding to Mal (**Fig. 7**). We incubated nickel bead–bound recombinant proteins with the cytoplasmic fraction of control neutrophils and evaluated the associations by immunoblot analysis with anti-Mal. Full-length Btk effectively bound to cytoplasmic Mal prepared from control neutrophils, but a control fusion of histidine-tagged Hph-1 and enhanced green fluorescent protein (eGFP) did not. Btk with deletion of the kinase domain almost completely lost the ability to interact with Mal, and Btk with deletion of the PH domain showed less binding to Mal. In contrast, recombinant proteins lacking the Tec homology domain, the Src homology 3 domain or the Src homology 2 domain had slightly greater capacity to associate with Mal (**Fig. 7b,d**). Other truncated Btk recombinant proteins without either the PH domain or kinase domain failed to bind to Mal (**Fig. 7c,d**), which suggested that both the PH domain and kinase domain are critical for the Btk-Mal interaction.

PTKs associate with Mal and regulate PI(3)K activation

The precise mechanism of PI(3)K activation triggered by membrane-associated Mal is largely unknown. As several PTKs were phosphorylated

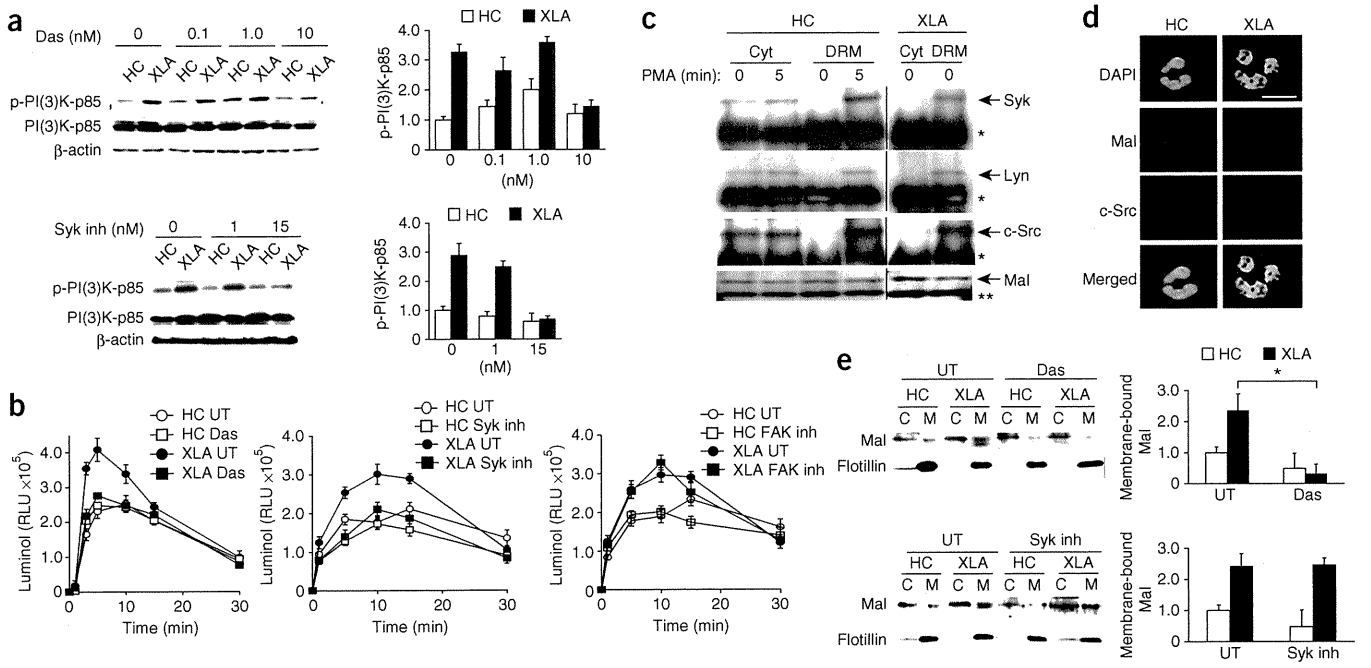

Figure 8 SFKs and Syk are involved in PI(3)K activation and the augmented production of ROS, whereas SFKs are involved in the membrane localization of Mal, in Btk-deficient neutrophils. (**a**) Immunoblot analysis (left of each pair) of total and phosphorylated PI(3)K-p85 in neutrophils from healthy controls and patients with XLA ($n = 4$ per group), treated with dasatinib (Das; at 10 nM, to inhibit the activity of c-Src, Lyn and Bcr-Abl but not FAK or Syk directly[36]) or a Syk inhibitor (Syk inh). Right (of each pair), densitometry of PI(3)K-p85 phosphorylated at Tyr508, presented as band intensity relative to that in untreated neutrophils from healthy controls, set as 1. (**b**) H_2O_2 production in neutrophils ($n = 4$ donors per group) left untreated (UT) or pretreated with dasatinib (10 nM), Syk inhibitor (15 nM) or FAK inhibitor (4 nM), and then stimulated with PMA, assessed by luminol assay and presented in relative light units (RLU). (**c**) Immunoassay of cytosolic fractions (Cyt) and detergent-resistant membrane fractions (DRM) of neutrophils from healthy controls and patients with XLA, left untreated (0) or treated for 5 min with PMA (5), followed by immunoprecipitation with anti-Mal and immunoblot analysis with anti-Syk, anti-Lyn, anti-c-Src or anti-Mal. *, immunoglobulin heavy chain; **, immunoglobulin light chain. (**d**) Confocal microscopy of neutrophils from healthy controls and patients with XLA ($n = 3$ per group), stained with anti-Mal (red) and anti-c-Src (blue) and counterstained with DAPI. Original magnification, ×600; scale bar, 10 μm. (**e**) Immunoblot analysis (left) of Mal in the cytoplasm (C) and membrane (M) of neutrophils from healthy controls and patients with XLA ($n = 5$ per group), left untreated or treated as in **a**. Right, quantification of results for Mal (left), presented relative to that of flotillin in the membrane fraction of neutrophils from healthy controls, set as 1. *$P = 0.0024$ (Student's *t*-test). (**f**) Immunoblot analysis of total Syk and Syk phosphorylated at Tyr524 and Tyr525 (top left) and of total c-Src and c-Src phosphorylated at Tyr416 (bottom left) in neutrophils from healthy controls and patients with XLA, left untreated or treated with dasatinib (top left) or Syk inhibitor (bottom left). Right, quantification of band intensity relative to that of β-actin in untreated neutrophils from healthy controls, set as 1. *$P = 0.013$ (Student's *t*-test). Data are from four (**a**) or five (**f**) independent experiments, are from one representative of four independent experiments (**c**) or are representative of four experiments (**b**,**e**) or three experiments (**c**; mean and s.d. in **a**,**b**,**e**,**f**).

in resting neutrophils from patients with XLA, we first used PTK inhibitors to investigate whether PTKs were involved in the PI(3)K activation. Inhibition of the activity of Src-family kinases (SFKs) by dasatinib (at a concentration of 10 nM)[36] led to normalized phosphorylation of PI(3)K-p85 in neutrophils derived from patients with XLA. Similarly, a Syk inhibitor (at a concentration of 15 nM)[37] but not a FAK inhibitor (at a concentration of 10 nM)[38] abrogated the hyperphosphorylation of PI(3)K (**Fig. 8a** and data not shown). The lower PI(3)K phosphorylation produced by dasatinib or the Syk inhibitor was accompanied by normalized production of ROS (**Fig. 8b**), which indicated that SFKs and Syk were involved in the augmented production of ROS in neutrophils from patients with XLA.

The findings noted above prompted us to determine whether the activated PTKs associated with Mal. SFKs are recruited to lipid rafts when activated for the assembly of signal components[39,40]. Coprecipitation assays showed that Lyn, c-Src and Syk interacted with Mal at the rafts of Btk-deficient neutrophils before stimulation (**Fig. 8c**). We also observed the colocalization of Mal and c-Src at the membrane by confocal fluorescence microscopy (**Fig. 8d**). We observed the interaction at the rafts of control neutrophils only after stimulation with PMA (**Fig. 8c** and **Supplementary Fig. 6**).

SFKs are cytoplasmic kinases and are anchored to the plasma membrane through myristoylation and palmitoylation[39,40]. Coprecipitation assays showed that Lyn, c-Src and Syk were associated with Mal in the cytosol of neutrophils from healthy controls but not in Btk-deficient neutrophils (**Fig. 8c**). We also confirmed by immunofluorescence staining the presence of c-Src associated with Mal in the cytoplasm but not in the membrane of normal resting neutrophils (**Fig. 8d**).

We next studied whether the membrane localization of Mal was regulated by SFKs or by Syk. The localization of Mal to the membrane in Btk-deficient neutrophils was diminished to normal amounts in cells treated with dasatinib but not those treated with the Syk inhibitor (**Fig. 8e**), which suggested that kinase activity of SFKs was required for membrane recruitment or maintenance of membrane-anchoring of Mal. Treatment of neutrophils from patients with XLA with dasatinib resulted in less baseline Syk phosphorylation, whereas incubation with the Syk inhibitor did not abrogate the hyperphosphorylation of c-Src (**Fig. 8f**), which indicated that Syk was downstream of SFKs in the steady-state signaling cascade of Btk-deficient neutrophils.

Collectively, the data reported above indicated that at least some PTKs associated with Mal together with Btk in the cytoplasm; in the absence of Btk, SFKs and Mal translocated to the membrane. The membrane-recruited PTKs formed a complex with and phosphorylated PI(3)K-p85 (**Supplementary Fig. 7**). It is still unclear which neutrophil SFK contributes to PI(3)K activation. Our findings may indicate that c-Src (or other SFKs) but not Lyn is (are) directly involved in the PI(3)K activation in Btk-deficient neutrophils; however, the possibility of an indirect contribution of Lyn to the phosphorylation of PI(3)K-p85 cannot be excluded solely by the inhibitor assay.

DISCUSSION

So far, most data have posited Btk as an essential molecule in innate immune responses[12–15,23,25]. Here we have shown that Btk is a negative regulator of signal transduction that leads to activation of NADPH oxidase and a molecule that prevents excessive neutrophil responses. Neutropenia in patients with XLA is usually induced by infection and is observed less often after immunoglobulin supplementation. This phenomenon can most probably be explained by ROS-mediated apoptosis of neutrophils triggered by the engagement of innate receptors and not by abnormal myeloid differentiation.

Our study suggested that Btk serves as a cytosolic component that interacts with Mal to prevent its translocation to the membrane and its interactions with PI(3)K until the appropriate stimulation is received. Both the PH and kinase domains of Btk were necessary for association with cytoplasmic Mal and were important for proper and coordinated initiation of the TLR and TNF receptor responses in human neutrophils. A similar mode of interaction has been demonstrated for the association of Btk with the cell-surface death receptor Fas (CD95) in B cells. Btk associates with Fas via its PH and kinase domains and prevents the interaction of Fas with the Fas-associated death domain and thus serves as a negative regulator of the Fas death-inducing signaling complex[41]. Notably, Btk serves as a negative regulator of apoptosis in both signaling systems.

SFKs were also involved in the baseline activation of PI(3)K in Btk-deficient neutrophils. We detected the association of c-Src, Lyn and Syk with Mal in the membrane raft in the absence of Btk. In addition, localization of Mal to the membrane in Btk-defective neutrophils was dependent on SFKs. These findings may indicate that SFKs serve as a substitute for the function of Btk in guiding the localization of Mal, albeit in an unregulated way. In neutrophils from control subjects, SFKs and Mal were associated in the cytoplasm and localized to the raft after stimulation. The mode of the SFK-Mal interaction remains unclear; however, we speculate that the kinase domain is involved, as SFKs lack a PH domain and the kinase domains of SFKs and Btk share 40–45% homology. Precise mapping of the Mal-binding site in the Btk kinase domain would help to clarify the SFK-Mal association site. Notably, neutrophils had more abundant expression of Mal than did monocytes (data not shown). Our data suggest that Mal is a critical coordinator of the priming signal and that its localization is tightly controlled by Btk.

Limited data indicate a role for PTKs in the production of ROS in neutrophils, particularly in humans. Lyn is reported to be a signaling component of the immunoglobulin receptors FcγRI and FcγRII or the receptor for the hematopoietic cytokine G-CSF, as well as an activator of PI(3)K[30,42], but is also noted for its ability to negatively regulate myeloid-cell signaling through phosphorylation of inhibitory receptors and recruitment of phosphatases[29]. Lyn-deficient neutrophils produce less ROS than Lyn-sufficient neutrophils do after stimulation with G-CSF[30] but show an enhanced respiratory burst after integrin-mediated signaling[29,31]. ROS responses triggered by *Aspergillus* species are totally dependent on Syk in mouse neutrophils[43]. The phosphorylation at different regulatory sites in Lyn versus c-Src in Btk-deficient neutrophils is notable. However, overall, PTKs in unstimulated neutrophils from patients with XLA seem to function as positive signal regulators. These data, along with our observations, suggest a potential contribution of SFKs and Syk to the early phase of NADPH oxidase activation in human neutrophils.

Activation of TFKs occurs downstream of SFKs in signaling pathways[40]. However, in neutrophils, Btk regulates baseline SFK activation. There are several possible mechanisms to explain how defective Btk is connected to SFK activation. We first speculated that Btk controls SFKs through the activation of negative SFK regulators. We investigated the Src kinase Csk and its regulatory molecule Cbp[44], but found no difference in the expression, localization or phosphorylation of Csk or Cbp (data not shown). As a second possible mechanism, SFKs but not TFKs may have been activated to compensate for Btk function in neutrophils. It is noteworthy that Btk regulates PtdIns(4,5)P_2 synthesis, acting as a shuttle to bring type I phosphatidylinositol-4-phosphate 5-kinases to the plasma membrane in B cells[45]. Although the role of Btk in PtdIns(4,5)P_2 production in human neutrophils has not been addressed, the generation of PtdIns(4,5)P_2 is a critical

step in the activation of NADPH oxidase. SFKs may have directly or indirectly served as a substitute for the function of Btk in neutrophils from patients with XLA. Finally, the cytoplasmic association of SFKs with Mal but without Btk may have resulted in SFK activation and Lyn inhibition. The phosphorylation of SFKs and subsequent modification of Mal by SFKs may have led to the translocation of Mal in the absence of Btk.

Neutrophils from patients with XLA show excessive production of ROS, but neutrophils from mice with X-linked immunodeficiency show poor ROS induction[15]. One possibility that could explain this discrepancy is the difference between mice and humans in the involvement of Btk in the NADPH oxidase pathway. Another possibility is the difference in the contributions of various members of the PI(3)K family to neutrophil activation. The primed production of ROS requires sequential activation of PI(3)Kγ and PI(3)Kδ in humans, whereas the production of ROS is largely dependent on PI(3)Kγ alone in mice[46]. A third possibility is differences in the methods of neutrophil collection from mice and in our study. Neutrophils collected from the peritoneum after treatment with thioglycolate broth may have been stimulated by that treatment[15]. The production of ROS was not augmented or compromised in neutrophils from patients with XLA in one study[26]. That may also have resulted from a relatively harsh isolation technique of hypotonic shock or from non–endotoxin-free conditions (for example, lipopolysaccharide in FBS) at any point of the experiment.

In this study, we have reported that Btk serves as a critical gatekeeper of neutrophil response. Our study suggests that the regulation of neutrophil activation and apoptosis in various human diseases could be achieved by manipulation of Btk. Future studies should explore the role of Btk in controlling the production of ROS and apoptosis of basophils, mast cells and eosinophils. Finally, ROS-mediated induction of apoptosis after suboptimal or optimal stimuli may be worth investigating in immature and precursor cells of the immune reponse to determine the role of Btk in their survival, proliferation and differentiation.

METHODS

Methods and any associated references are available in the online version of the paper at http://www.nature.com/natureimmunology/.

Note: Supplementary information is available on the Nature Immunology website.

ACKNOWLEDGMENTS

We thank E. Tsitsikov, E. Rachlin, K. Imai and J. Yata for discussions; all patients who participated in this study; S. Goo Rhee (Ewha Womans University) for antibody to Prx1 phosphorylated at Tyr194; and J.A. Lindquist (Otto-von-Guericke University) for antibody to Cbp (PAG) phosphorylated at Tyr317. Supported by the Ministry of Health, Labour and Welfare of Japan (H. Kane, S.N. and T.M.), the Ministry of Education, Culture, Sports, Science and Technology of Japan (S.M. and T.M.) and by the National Research Foundation of Korea (National Creative Research Initiatives grant to S.-K.L.).

AUTHOR CONTRIBUTIONS

F.H. did experiments; E.-S.K. and S.-K.L. contributed to protein-delivery experiments and provided some technical support; H. Kano and H. Kane made suggestions on data analysis and interpretation; S.N. and S.M. provided advice on project planning and data interpretation; M.T. provided advice on project plan and edited the manuscript; T.M. directed the project, designed research and wrote the manuscript; and all authors reviewed and approved the manuscript.

COMPETING FINANCIAL INTERESTS

The authors declare no competing financial interests.

Published online at http://www.nature.com/natureimmunology/.
Reprints and permissions information is available online at http://www.nature.com/reprints/index.html.

1. Flannagan, R.S., Cosio, G. & Grinstein, S. Antimicrobial mechanisms of phagocytes and bacterial evasion strategies. *Nat. Rev. Microbiol.* **7**, 355–366 (2009).
2. Nauseef, W.M. How human neutrophils kill and degrade microbes: an integrated view. *Immunol. Rev.* **219**, 88–102 (2007).
3. Lambeth, J.D. NOX enzymes and the biology of reactive oxygen. *Nat. Rev. Immunol.* **4**, 181–189 (2004).
4. Babior, B.M. NADPH oxidase. *Curr. Opin. Immunol.* **16**, 42–47 (2004).
5. Sumimoto, H. Structure, regulation and evolution of Nox-family NADPH oxidases that produce reactive oxygen species. *FEBS J.* **275**, 3249–3277 (2008).
6. Fang, F.C. Antimicrobial reactive oxygen and nitrogen species: concepts and controversies. *Nat. Rev. Microbiol.* **2**, 820–832 (2004).
7. Singh, A., Zarember, K.A., Kuhns, D.B. & Gallin, J.I. Impaired priming and activation of the neutrophil NADPH oxidase in patients with IRAK4 or NEMO deficiency. *J. Immunol.* **182**, 6410–6417 (2009).
8. Woollard, K.J. & Geissmann, F. Monocytes in atherosclerosis: subsets and functions. *Nat. Rev. Cardiol.* **7**, 77–86 (2009).
9. Finkel, T. Radical medicine: treating ageing to cure disease. *Nat. Rev. Mol. Cell Biol.* **6**, 971–976 (2005).
10. Conley, M.E. *et al.* Genetic analysis of patients with defects in early B-cell development. *Immunol. Rev.* **203**, 216–234 (2005).
11. Winkelstein, J.A. *et al.* X-linked agammaglobulinemia: report on a United States registry of 201 patients. *Medicine (Baltimore)* **85**, 193–202 (2006).
12. Mohamed, A.J. *et al.* Bruton's tyrosine kinase (Btk): function, regulation, and transformation with special emphasis on the PH domain. *Immunol. Rev.* **228**, 58–73 (2009).
13. Gray, P. *et al.* MyD88 adapter-like (Mal) is phosphorylated by Bruton's tyrosine kinase during TLR2 and TLR4 signal transduction. *J. Biol. Chem.* **281**, 10489–10495 (2006).
14. Doyle, S.L., Jefferies, C.A., Feighery, C. & O'Neill, L.A. Signaling by Toll-like receptors 8 and 9 requires Bruton's tyrosine kinase. *J. Biol. Chem.* **282**, 36953–36960 (2007).
15. Mangla, A. *et al.* Pleiotropic consequences of Bruton tyrosine kinase deficiency in myeloid lineages lead to poor inflammatory responses. *Blood* **104**, 1191–1197 (2004).
16. Fiedler, K. *et al.* Neutrophil development and function critically depend on Bruton tyrosine kinase in a mouse model of X-linked agammaglobulinemia. *Blood* **117**, 1329–1339 (2011).
17. Conley, M.E. *et al.* Primary B cell immunodeficiencies: comparisons and contrasts. *Annu. Rev. Immunol.* **27**, 199–227 (2009).
18. Kerner, J.D. *et al.* Impaired expansion of mouse B cell progenitors lacking Btk. *Immunity* **3**, 301–312 (1995).
19. Khan, W.N. *et al.* Defective B cell development and function in Btk-deficient mice. *Immunity* **3**, 283–299 (1995).
20. O'Neill, L.A.J. & Bowie, A.G. The family of five: TIR-domain-containing adaptors in Toll-like receptor signalling. *Nat. Rev. Immunol.* **7**, 353–364 (2007).
21. Piao, W. *et al.* Tyrosine phosphorylation of MyD88 adapter-like (Mal) is critical for signal transduction and blocked in endotoxin tolerance. *J. Biol. Chem.* **283**, 3109–3119 (2008).
22. Jenkins, K.A. & Mansell, A. TIR-containing adaptors in Toll-like receptor signalling. *Cytokine* **49**, 237–244 (2010).
23. Taneichi, H. *et al.* Toll-like receptor signaling is impaired in dendritic cells from patients with X-linked agammaglobulinemia. *Clin. Immunol.* **126**, 148–154 (2008).
24. Pérez de Diego, R. *et al.* Bruton's tyrosine kinase is not essential for LPS-induced activation of human monocytes. *J. Allergy Clin. Immunol.* **117**, 1462–1469 (2006).
25. Horwood, N.J. *et al.* Bruton's tyrosine kinase is required for TLR2 and TLR4-induced TNF, but not IL-6, production. *J. Immunol.* **176**, 3635–3641 (2006).
26. Marron, T.U., Rohr, K., Martinez-Gallo, M., Yu, J. & Cunningham-Rundles, C. TLR signaling and effector functions are intact in XLA neutrophils. *Clin. Immunol.* **137**, 74–80 (2010).
27. Honda, F. *et al.* Transducible form of p47phox and p67phox compensate for defective NADPH oxidase activity in neutrophils of patients with chronic granulomatous disease. *Biochem. Biophys. Res. Commun.* **417**, 162–168 (2012).
28. Dang, P.M. *et al.* A specific p47phox -serine phosphorylated by convergent MAPKs mediates neutrophil NADPH oxidase priming at inflammatory sites. *J. Clin. Invest.* **116**, 2033–2043 (2006).
29. Scapini, P., Pereira, S., Zhang, H. & Lowell, C.A. Multiple roles of Lyn kinase in myeloid cell signaling and function. *Immunol. Rev.* **228**, 23–40 (2009).
30. Zhu, Q.S. *et al.* G-CSF induced reactive oxygen species involves Lyn-PI3-kinase-Akt and contributes to myeloid cell growth. *Blood* **107**, 1847–1856 (2006).
31. Pereira, S. & Lowell, C. The Lyn tyrosine kinase negatively regulates neutrophil integrin signaling. *J. Immunol.* **171**, 1319–1327 (2003).
32. Vlahos, C.J., Matter, W.F., Hui, K.Y. & Brown, R.F. A specific inhibitor of phosphatidylinositol 3-kinase, 2-(4-morpholinyl)-8-phenyl-4H–1-benzopyran-4-one (LY294002). *J. Biol. Chem.* **269**, 5241–5248 (1994).
33. Sadhu, C., Masinovsky, B., Dick, K., Sowell, C.G. & Staunton, D.E. Essential role of phosphoinositide 3-kinase δ in neutrophil directional movement. *J. Immunol.* **170**, 2647–2654 (2003).
34. Morris, A.C. *et al.* C5a-mediated neutrophil dysfunction is RhoA-dependent and predicts infection in critically ill patients. *Blood* **117**, 5178–5188 (2011).
35. Santos-Sierra, S. *et al.* Mal connects TLR2 to PI3Kinase activation and phagocyte polarization. *EMBO J.* **28**, 2018–2027 (2009).

36. Nam, S. *et al.* Action of the Src family kinase inhibitor, dasatinib (BMS-354825), on human prostate cancer cells. *Cancer Res.* **65**, 9185–9189 (2005).
37. Lai, J.Y. *et al.* Potent small molecule inhibitors of spleen tyrosine kinase (Syk). *Bioorg. Med. Chem. Lett.* **13**, 3111–3114 (2003).
38. Slack-Davis, J.K. *et al.* Cellular characterization of a novel focal adhesion kinase inhibitor. *J. Biol. Chem.* **282**, 14845–14852 (2007).
39. Korade-Mirnics, Z. & Corey, S.J. Src kinase-mediated signaling in leukocytes. *J. Leukoc. Biol.* **68**, 603–613 (2000).
40. Bradshaw, J.M. The Src, Syk, and Tec family kinases: distinct types of molecular switches. *Cell. Signal.* **22**, 1175–1184 (2010).
41. Vassilev, A., Ozer, Z., Navara, C., Mahajan, S. & Uckun, F.M. Bruton's tyrosine kinase as an inhibitor of the Fas/CD95 death-inducing signaling complex. *J. Biol. Chem.* **274**, 1646–1656 (1999).
42. Wang, A.V., Scholl, P.R. & Geha, R.S. Physical and functional association of the high affinity immunoglobulin G receptor (FcγRI) with the kinases Hck and Lyn. *J. Exp. Med.* **180**, 1165–1170 (1994).
43. Boyle, K.B. *et al.* Class IA phosphoinositide 3-kinase β and δ regulate neutrophil oxidase activation in response to *Aspergillus fumigatus* hyphae. *J. Immunol.* **186**, 2978–2989 (2011).
44. Kawabuchi, M. *et al.* Transmembrane phosphoprotein Cbp regulates the activities of Src-family tyrosine kinases. *Nature* **404**, 999–1003 (2000).
45. Saito, K. *et al.* BTK regulates PtdIns-4,5-P2 synthesis: importance for calcium signaling and PI3K activity. *Immunity* **19**, 669–678 (2003).
46. Condliffe, A.M. *et al.* Sequential activation of class IB and class IA PI3K is important for the primed respiratory burst of human but not murine neutrophils. *Blood* **106**, 1432–1440 (2005).
47. Uckun, F.M. *et al.* Anti-breast cancer activity of LFM-A13, a potent inhibitor of Polo-like kinase (PLK). *Bioorg. Med. Chem.* **15**, 800–814 (2007).
48. Mahajan, S. *et al.* Rational design and synthesis of a novel anti-leukemic agent targeting Bruton's tyrosine kinase (BTK), LFM-A13 [alpha-cyano-β-hydroxy-β-methyl-N-(2,5-dibromophenyl)propenamide]. *J. Biol. Chem.* **274**, 9587–9599 (1999).

ONLINE METHODS

Reagents and antibodies. The following reagents were used: lipopolysaccharide derived from *Escherichia coli* or *Pseudomonas aeruginosa*, fMLP, PMA, DHR123, luminol, N-acetyl cysteine, aprotinin, leupeptin, pepstatin and phenylmethyl sulfonyl fluoride (all from Sigma-Aldrich); recombinant human TNF (R&D Systems); Pam_3CSK_4, LFM-A13, LFM-A11, Syk inhibitor, FAK inhibitor and Ly294002 (all from Calbiochem); and dasatinib, IC87114 and AS-605240 (all from Biovision). Oligodeoxynucleotide CpG-A (5′-GGT GCATCGATGCAGGGGGG-3′) was from Operon Biotechnologies.

The antibodies used were as follows: goat polyclonal antibody to PI(3)K-p85α phosphorylated at Tyr508 (sc-12929), Hck phosphorylated at Tyr411 (sc-12928), rabbit polyclonal antibody to Hck (N-30), anti-PTEN (FL-403), anti-PTP-PEST (H130), anti-FAK (A-17), anti-Vav (C-14), anti-Syk (C-20), anti-SHP2 (C-18) and anti-SHP 1 (C-19), as well as mouse monoclonal antibody (mAb) to $p47^{phox}$ (D-10), $p40^{phox}$ (D-8) or $p22^{phox}$ (CS-9; all from Santa Cruz). Rabbit polyclonal antibody to p101-PI(3)K (07-281) and to $gp91^{phox}$ (07-024) and anti-Rac2 (07-604), biotin-labeled mouse mAb to phosphorylated tyrosine (4G10), as well as horseradish peroxidase–conjugated antibody to goat IgG (AP-180P) were from Upstate; fluorescein isothiocyanate–conjugated mouse mAb to gp91 (7D5) or goat antibody to mouse IgG (238) were from MBL; and mouse mAb to flotillin-1(18), $p67^{phox}$ (29) or PI(3)K-p85 (U15), and fluorescein isothiocyanate–conjugate mouse isotype-matched IgG antibody (MOPC-21) was from BD Pharmingen. Rabbit polyclonal antibody to PI(3)K-p85 (4292), to Lyn (2732), to Lyn phosphorylated at Tyr507 (2731), to Syk phosphorylated Tyr525-Tyr526 (2711), to Src phosphorylated Tyr416 (2101), to FAK phosphorylated Tyr576-Tyr577 (3281), to $p40^{phox}$ phosphorylated at Thr154 (4311) and to caspase-3 (9662), as well as mouse mAb to proliferating cell nuclear antigen (PC-19), were from Cell Signaling. Rabbit mAb to SOD1 (ep1727y), Mal (ep1231y) and catalase (ep1929), as well as rabbit polyclonal antibody to SOD2 (NB100-1992) and to Yes (NBP1-85369), were from Novus Biologicals. Rabbit polyclonal antibody to Bmx (ab73887), to Bmx phosphorylated at Tyr566 (ab59409), to Lyn phosphorylated at Tyr396 (EP503Y), to Vav phosphorylated at Tyr160 (ab4763) and to Prx1 (ab15571), and mouse mAb to Prx2 (12B1), as well as rabbit mAb to Btk (Y440), to CSK (CSK-04), to SHIP (EP378Y) and to Tec (Y398), were from Abcam. Rat mAb to Mal (TIRAP; sebi-1) was from ENZO Life Sciences. Goat polyclonal antibody to CBP (LS-C14699) was from LIFESPAN; anti-β-actin (Ab1) was from Calbiochem; and horseradish peroxidase–conjugated antibody to mouse IgG (NA931), to rabbit IgG (NA934) or to rat IgG (NA9350) was from GE Healthcare. Alexa Flour 546–anti–rabbit IgG (A11035), Alexa Flour 680–anti–rabbit IgG (A10043), Alexa Flour 594–anti–rat IgG (A21209) and Alexa Flour 488–anti–mouse IgG (A21202) were from Invitrogen. Mouse IgG (015-000-003) and rabbit IgG (011-00000-3) were from Jackson ImmunoResearch. Rat IgG2a (eBR2a) was from eBioscience. Horseradish peroxidase–conjugated streptavidin was from Cell Signaling.

The 482H mAb to Btk has been described[49]. Polyclonal antibody to human Btk was raised in rabbits with a Btk peptide of amino acids 169–187 (ENRNGSLKPGSSHRKTKKPC) conjugated to ovalubumin. The antibody collected was further affinity-purified with that same Btk peptide conjugated to thiol–Sepharose 4B (Pharmacia) and was used for immunoprecipitation in some experiments. The specificity of the antibody was confirmed by immunoblot analysis of lysates of Btk-deficient mononuclear cells. Antibody to phosphorylated Ser345 was generated in rabbits by injection of ovalbumin conjugated to a peptide of $p47^{phox}$ phosphorylated at Ser345 (QARPGPQSpPGSPLEEE, where 'Sp' indicates phosphorylated Ser345 (p-Ser345-pep)). The antibody raised was positively affinity-purified with activated thiol–Sepharose 4B adsorbed with p-Ser345-pep. The antibody was further purified by elimination of the fraction that bound to the same peptide of $p47^{phox}$ without phosphorylation at Ser345 (QARPGPQSPGSPLEEE (Ser345-pep)) by passage through thiol–Sepharose 4B conjugated to Ser345-pep; then, the antibody was used for immunoblot analysis. The specificity of the antibody was confirmed by direct enzyme-linked immunosorbent assay with plates coated with Ser345-pep or p-Ser345-pep and by immunoblot analysis experiments showing blockade of the p-$p47^{phox}$ signal by p-Ser345pep but not by Ser345-pep.

Subjects. Patients with XLA (n = 17) with stable health were studied (ages and Btk mutations, **Supplementary Fig. 3**). Healthy volunteers (n = 18) and patients with CVID (n = 5) were enrolled as healthy controls and disease control, respectively. Written informed consent was obtained from all subjects (or their parents). The study protocol was approved by the ethics committee of the Faculty of Medicine, Tokyo Medical and Dental University.

Isolation of neutrophils, monocytes and lymphocytes. Neutrophils were purified from heparinized peripheral blood by a standard technique. All samples were processed within 12 h of blood collection. Peripheral blood diluted in PBS was layered onto a MonoPoly mixture (Flow Laboratories) and centrifuged at 400*g* for 20 min. Layers with enrichment for neutrophils were collected and further purified to a purity of >97% by immunomagnetic negative selection (StemCell Technologies). Sterile and endotoxin-free conditions were used for all procedures. Monocytes were purified from the mononuclear cell–rich fraction with a human monocyte enrichment kit (StemCell Technologies), and lymphocytes were prepared as described[50].

Measurement of production of ROS. Purified neutrophils were loaded for 5 min at 37 °C with DHR123 (5 μg/ml). Cells were washed and then stimulated for 30 min at 37 °C with PMA (100 ng/ml), and the production of ROS was quantified via flow cytometry by measurement of intracellular rhodamine (FACSCalibur; Becton Dickinson). DHR123-loaded neutrophils were also stimulated for 60 min at 37 °C with a TLR ligand (lipopolysaccharide from *E. coli* or *P. aeruginosa*; 100 ng/ml), CpG-A (100 ng/ml) or TNF (1 μg/ml). After incubation, treated and untreated neutrophils were incubated for 5 min at 37 °C with or without fMLP (1 μM), followed by flow cytometry. Results are presented as MFI of treated cells – MFI of untreated cells.

Production of ROS was quantified by standard chemiluminescence. Neutrophils (1.0×10^6) were suspended in 0.5 ml PBS containing luminol (10 μM) preheated to 37 °C. After a baseline measurement was obtained, cells were stimulated with a TLR agonist and then with fMLP (1 μM) or with PMA (100 ng/ml); luminescence signals were monitored throughout the reaction.

Detection of apoptosis. Apoptotic cells were identified by staining with annexin V–fluorescein isothiocyanate and 7-AAD (7-amino-actinomycin D; BD Biosciences). Apoptosis was also identified by immunoblot analysis through the detection of cleaved caspase-3 or degraded proliferating cell nuclear antigen.

Flow cytometry. A FACSCalibur (Beckton Dickenson) was used for all flow cytometry analyzing surface expression of gp91, DHR123 staining, annexin V–7-AAD staining, and JC-1 mitochondrial membrane detection as described[50]. All analyses were undertaken after calibration of the fluorescence intensity with CaliBRITE Beads (BD Biosciences).

Subcellular fractionation of neutrophils. Isolated neutrophils were resuspended at a density of 5×10^7 cells per ml in ice-cold sonication buffer (HEPES (10 mM), pH 7.2, sucrose (0.15 M), EGTA (1 mM), EDTA (1 mM), NaF (25 mM), leupeptin (10 μg/ml), pepstatin (10 μg/ml), aprotinin (1 μg/ml) and PMSF (1 mM)). After sonication and pelleting on ice, 200 μl supernatant was layered on a discontinuous sucrose gradient consisting of 200 μl of 52% (wt/vol) sucrose, 200 μl of 40% (wt/vol) sucrose and 200 μl of 15% (wt/vol) sucrose. After centrifugation (100,000*g* for 60 min), 160 μl supernatant (cytosol source) and 120 μl interface of the 15%–40% sucrose layers (plasma-membrane source) were collected.

Immunoprecipitation and immunoblot analysis. Lysates were prepared from monocytes and lymphocytes as described[51]. For the preparation of lysates from neutrophils, cells were resuspended in lysis buffer (Tris-HCl (50 mM), pH 7.5, NaCl (150 mM), sucrose (0.25 M), EGTA (5 mM), EDTA (5 mM), leupeptin (15 μg/ml), pepstatin (10 μg/ml), aprotinin (10 μg/ml), PMSF (2.5 mM), 1.0% Nonidet-P40, 0.25% sodium deoxycholate, sodium pyrophosphate (10 mM), NaF (25 mM), Na_3VO_4 (5 mM), β-glycerophosphate (25 mM) and DNase I (1 μg/ml)), incubated for 30 min on ice and centrifuged at 15,000*g* for 30 min at 4 °C, then supernatants were collected. For extraction of the membrane-raft fraction, 1% n-dodecyl-β-D-maltoside was added to the lysis buffer. Immunoprecipitation and immunoblot analysis were done as described[52]. For immunoprecipitation of cytosolic proteins from neutrophils, cytosolic proteins

obtained as described above were diluted in four volumes of immunoprecipitation buffer (Tris-HCl (20 mM), pH 7.5, NaCl (150 mM), sucrose (0.25 M), EGTA (5 mM), EDTA (5 mM), leupeptin (15 μg/ml), pepstatin (10 μg/ml), aprotinin (10 μg/ml), PMSF (2.5 mM), 0.5% Triton-X, sodium pyrophosphate (10 mM), NaF (25 mM), Na_3VO_4 (5 mM), β-glycerophosphate (50 mM) and levamisole (1 mM)); supernatants were used for immunoprecipitation.

Measurement of phosphatidylinositol-(3,4,5)-trisphosphate. Phosphatidylinositol-(3,4,5)-trisphosphate in unstimulated neutrophils prepared from healthy controls and patients with XLA was measured with an enzyme-linked immunosorbent assay kit in accordance with the manufacturer's instructions (K-2500; Echelon).

Immunofluorescence staining. Cytospin preparations of neutrophils were air-dried and fixed for 10 min with paraformaldehyde in PBS, pH 7.4, then were made permeable for 20 min at −20 °C with acetone, washed, and incubated with the appropriate antibodies. After labeling and washing with 0.2% BSA in PBS, coverslips were mounted with Fluoromount G and the prepared specimens. Nuclei were counterstained with DAPI (4,6-diamidino-2-phenylindole). Slides were analyzed with a fluorescence microscope (FV10i; Olympus) equipped with Fluoview viewer and review station (Olympus). At least 100 cells were inspected for each slide.

Generation of Hph-1-Btk, Hph-1-Btk mutants, and transduction of recombinant protein into cells. Hph-1–tagged Btk constructs were generated by amplification of a full-length Btk cDNA fragment with the appropriate primers (**Supplementary Table 1a**). After the sequence of each PCR product was verified by DNA sequencing, the fragment was ligated into sites of a pET28b vector (Merck) cleaved by *Xma1* and *Sal1*; the vector has a six-histidine site for protein purification and two tandem Hph-1 sequences for protein transduction. Constructs with deletion of the Tec homology domain, SH3 domain or SH2 domain were generated by mutagenesis with the QuikChange SiteDirected Mutagenesis Kit (Stratagene) and the appropriate primers (**Supplementary Table 1b**). The Hph-1-Gal4 construct has been described[52]. Proteins were induced in BL21 Star competent cells (Novagen) as described[52]. Proteins were treated with Detoxi-Gel Endotoxin Removing Gel (Takara Bio) for elimination of endotoxins and were frozen at −80 °C until further use. Neutrophils (1×10^6 per ml) were incubated for 1 h with 1 μM Hph-1–tagged proteins (80 μg recombinant Hph-1–tagged full-length-Btk was used for 1×10^6 neutrophils for transduction at a concentration of 1 μM) and washed, then ROS production was assayed.

Btk-precipitation assay. Lysates of neutrophils from healthy controls were prepared on ice for 30 min with immunoprecipitation lysis buffer. Supernatants were then treated with protein G beads (GE Health Care) for removal of immunoglobulin G from the neutrophil lysate. For the Btk-precipitation assay, purified Btk recombinant proteins or control recombinant protein were eluted and proteins were measured by BCA protein assay (Pierce). Bacterial supernatants were bound to nickel–nitrilotriacetic acid Sepharose beads (Qiagen) and bound recombinant proteins were eluted, then equimolar amounts of recombinant proteins were rebound to the nickel beads; afterward, samples were washed and then incubated overnight at 4 °C with the cell lysates. Beads were washed four times with lysis buffer and assessed by immunoblot analysis with anti-Mal. Before incubation with cell lysates, the amount of the recombinant protein rebound to nickel beads was assessed by immunoblot analysis with anti-histidine, and the 'dose' was readjusted for further precipitation assays.

Statistical analysis. Student's *t*-test was used for statistical analysis. The software GraphPad Prism 4 was used for these analyses.

49. Futatani, T. *et al.* Deficient expression of Bruton's tyrosine kinase in monocytes from X-linked agammaglobulinemia as evaluated by a flow cytometric analysis and its clinical application to carrier detection. *Blood* **91**, 595–602 (1998).
50. Takahashi, N. *et al.* Impaired CD4 and CD8 effector function and decreased memory T cell populations in ICOS-deficient patients. *J. Immunol.* **182**, 5515–5527 (2009).
51. Morio, T. *et al.* Ku in the cytoplasm associates with CD40 in human B cells and translocates into the nucleus following incubation with IL-4 and anti-CD40 mAb. *Immunity* **11**, 339–348 (1999).
52. Choi, J.M. *et al.* Intranasal delivery of the cytoplasmic domain of CTLA-4 using a novel protein transduction domain prevents allergic inflammation. *Nat. Med.* **12**, 574–579 (2006).

doi:10.1038/ni.2234

Int J Hematol (2012) 95:299–310
DOI 10.1007/s12185-012-1013-1

ORIGINAL ARTICLE

Impaired cell adhesion, apoptosis, and signaling in WASP gene-disrupted Nalm-6 pre-B cells and recovery of cell adhesion using a transducible form of WASp

Rikiya Sato · Susumu Iizumi · Eun-Sung Kim · Fumiko Honda · Sang-Kyou Lee · Noritaka Adachi · Hideki Koyama · Shuki Mizutani · Tomohiro Morio

Received: 7 October 2011 / Revised: 18 January 2012 / Accepted: 19 January 2012 / Published online: 5 February 2012

Abstract Wiskott–Aldrich syndrome (WAS) is an X-linked immunodeficiency disease affecting cell morphology and signal transduction in hematopoietic cells. The function of Wiskott–Aldrich syndrome protein (WASp) and its partners in protein interaction have been studied intensively in mice; however, detailed biochemical characterization of its signal transduction and assessment of its functional consequence in human WASp-deficient lymphocytes remain difficult. In this study, we generated Nalm-6 cells in which the WAS protein gene (WASP) was disrupted by homologous recombination-based gene targeting and a cell-permeable form of recombinant WASp for functional study. The $WASP^{-/-}$ cells showed impaired adhesive capacity and polarization to plate-bound anti-CD47 mAb, anti-CD9 mAb, or to fibronectin. The defective morphological changes were accompanied by impaired intracellular signaling. In addition, the WASp-deficient cells displayed augmented apoptosis induced by CD24 cross-linking. A recombinant fusion protein composed of Hph-1 cell-permeable peptide and WASp prepared in *Escherichia coli*. Hph-1-WASp was efficiently transduced and expressed in $WASP^{-/-}$ Nalm-6 cells in a dose-dependent manner. The wild-type WASp, but not the mutant restored adhesion capacity, spreading morphology, and cytoskeletal reorganization. Additionally, the recombinant protein was successfully transduced into normal lymphocytes. These findings suggest that gene-disrupted model cell lines and cell-permeable recombinant proteins may serve as important tools for the detailed analysis of intracellular molecules involved in PID.

Keywords Wiskott–Aldrich syndrome · Gene targeting · Protein transduction domain · Gene therapy

R. Sato · F. Honda · S. Mizutani · T. Morio (✉)
Department of Pediatrics and Developmental Biology, Tokyo Medical and Dental University Graduate School of Medicine, 1-5-45 Yushima, Bunkyo-ku, Tokyo 113-8519, Japan
e-mail: tmorio.ped@tmd.ac.jp

S. Iizumi · N. Adachi · H. Koyama
Kihara Institute for Biological Research, Graduate School of Integrated Science, Yokohama City University, 641-12 Maioka-cho, Totsuka-ku, Yokohama 224-0813, Japan

E.-S. Kim · S.-K. Lee
Department of Biotechnology, College of Life Science and Biotechnology, National Creative Research Initiatives Center For Inflammatory Response Modulation, Yonsei University, 134 ShinChon-dong, SoDaeMun-gu, Seoul 120-749, South Korea

Introduction

Wiskott–Aldrich syndrome (WAS) is an X-linked immunodeficiency disease characterized by thrombocytopenia with small platelet volume, eczema, and recurrent infections [1, 2]. WAS is caused by a variety of mutations in the WAS protein (WASp) gene (*WASP*) which is expressed in cells of hematopoietic origin [3–5]. WASp is a member of a distinct family of proteins that participates in transduction of signals from the cell surface to the actin cytoskeleton. Defect related to WASp lead to faulty cell migration, proliferation, and survival [6–9].

The structure and functional biochemistry of WASp has been extensively studied. WASp has several principal domains that regulate its function and subcellular localization. These include a WH1 domain, a basic region, a GTPase-binding domain, a proline-rich region, a verprolin homology domain, a central domain, and an acidic domain. The WH1 domain of WASp interacts with WIP, a protein

that stabilizes WASp-regulated actin filaments, and is important for filopodium formation [10, 11]. The proline-rich region of WASp is required for optimal actin-polymerization activity. The region provides binding sites for SH3 domain containing proteins, including adaptor proteins (CIP4, Nck, Grb2, PSTPIP, and intersectin-2) and tyrosine kinases (Fyn, Lyn, Hck, and Btk), which may phosphorylate and activate WASp [6–9, 12–15]. One of the key mechanisms of WASp activation is through specific interaction of a Cdc42- and Rac-interactive binding domain of WASp with GTP-bound Cdc42. Cdc42 regulates the formation of filopodium formation and cell–substrate adhesions, and controls cell polarity and motility [9, 16, 17].

Functional and biochemical analysis of WASp-deficient immune cells has been explored using splenic cells of *Wasp*-disrupted mice, an Epstein–Barr virus-transformed lymphoblastoid cell line (EBV-LCL), human T-cell leukemia virus type 1 (HTLV-1)-transformed T lymphocytes, and peripheral blood lymphocytes from human WAS patients. $WASP^{-/-}$ T cells fail to reorganize actin filaments in response to T-cell receptor engagement, and are defective in forming cell-activating immunological synapses. T-cell signaling is impaired in WASp-deficient cells, leading to incomplete cell activation and abnormal proliferation. T cells from patients with WAS also display aberrant expression of surface antigens, including downregulation of sialylated surface proteins such as CD43, CDw75, and CD76 surface determinants generated by β-galactoside α-2,6 sialyl transferase [18]. Although previous data show abnormal cell morphology as well as impaired receptor capping and surface marker expression in WASp-deficient B cells [19], a detailed biochemical study of human B cells has been difficult and yet to be explored [19–26].

In this study, we examined the functional and biochemical defects of human B cells by generating a WASp-deficient B-cell line: *WASP* gene was disrupted in a human pre-B-cell line, Nalm-6, by homologous recombination for in-depth analysis of morphological change and actin reorganization induced by signal through various receptors. To generate the model cell line, we used a simplified vector construction system and a high-efficiency gene-targeting method, which enables rapid disruption of any locus of the human genome in a short period of time [27, 28].

Practical gene/protein correction systems should permit detailed biochemical and functional studies of a particular molecule in immune cells involved in human primary immunodeficiency disease. One frequently used method is a retrovirus-mediated gene transduction system; however, this technique is still labor intensive and has difficulties related to controllable protein expression. A minimally toxic and efficient intracellular WASp delivery system would allow detailed functional studies of cell lines as well as primary cells. In this study, we employed protein delivery through a novel cell-permeable protein transduction domain (PTD) for functional reconstitution assay in the *WASP*-disrupted cells. The peptide is from the human transcription factor Hph-1 [29], and has transduction efficiency comparable to TAT (the protein transduction domain of transactivating transcription polypeptide), minimal toxicity, and reasonable stability in vitro and in vivo.

We here report our findings with regard to the cell adhesion and protrusion induced by CD47 engagement, CD9 crosslinking, or by fibronectin, and cell apoptosis induced by CD24 crosslinking in the WASp-deficient cells. We studied differences in tyrosine phosphorylation of protein tyrosine kinases (PTKs) elicited by the engagement of CD47 and CD9 between wild-type (wt) and WASp-deficient Nalm-6 cells. A fusion protein composed of Hph-1 and full-length WASp, but not mutant recombinant WASp, complemented cellular dysfunction caused by the *WASP* mutation.

Materials and methods

Construction of targeting vectors

Construction of targeting vectors was performed as described previously [28]. Briefly, 1.8- and 2.3-kb genomic fragments were obtained by PCR with Platinum PCR SuperMix High Fidelity (Invitrogen Japan, Tokyo, Japan) using genomic DNA from healthy donors as a template, verified by DNA sequencing, and were used as 5′ and 3′ arms, respectively, in a pDONR vector. The primer sequences used for the 5′ arm were 5′-GGGGACAACTTT GTATAGAAAAGTTGGCCTCGCCAGAGAAGACAAG-3′ and 5′-GGGGACTGCTTTTTTGTACAAACTTGAGTAC AGCTCCTGTTCCCAGA-3′, and those for the 3′ arm were 5′-GGGGACAGCTTTCTTGTACAAAGTGGCCAC TCCCTCCTGCTCTG-3′ and 5′-GGGGACAACTTTGT ATAATAAAGTTGTGAGTGTGAGGACCAGGCAG-3′. Using MultiSite Gateway® Technology (Invitrogen Japan), a floxed Puro^r gene was inserted between the 5′ and 3′ arms on a plasmid carrying a diphtheria toxin A gene.

Cell line and transfection

EBV-LCL was established from healthy donors and from patients with WAS. Studies using the patients' cell lines were approved by the institutional ethical committee. Human Nalm-6 cells of pre-B-cell origin with an XY karyotype were cultured in ES medium (Nissui Seiyaku, Tokyo, Japan) supplemented with 10% fetal calf serum (FCS) and 50 μM 2-mercaptoethanol. DNA transfection

was carried out as described previously [27, 28]. Briefly, 4×10^6 cells were electroporated with 1.65 μg of targeting vector linearized with *Pme*I in a 40-μL chamber of Electro Gene Transfer Equipment (GTE-1; Shimadzu, Kyoto, Japan). After a 22-h incubation, the cells were incubated for an additional 2 weeks at 37°C in 0.15% agarose medium containing 0.5 μg/mL puromycin. Genomic DNA was isolated from drug-resistant colonies and subjected to PCR analysis. The cell lysates were analyzed by anti-WASp immunoblot.

PCR analysis of drug-resistant clones

Genomic DNA isolated from puromycin-resistant colonies was screened by PCR using a primer from a promoter region of the WASP gene (5′-TTTACTGTAGTAACCCTT CCGGACT-3′) and a primer (5′-AATAATGGTTTCTTA GACGTGCG-3′) located between the attL1 and lox-P sequences of Puro^r.

Cell aggregation assay

For assessing cell aggregation through CD9 engagement, cells were incubated at 3×10^5/mL with anti-CD9 mAb (ALB6) at 0.5 μg/mL in 24-well flat-bottomed plates (BD Falcon) for 48 h, and inspected under a microscope.

Cell adhesion and polarization assay

For this procedure, 96-well flat-bottomed plates were precoated with anti-CD47 mAb or with anti-CD9 mAb at 10 μg/mL in 100 μL of 0.1 M NaHCO3 buffer (pH 9) overnight at 4°C, and then washed and blocked with 5% FCS/PBS. Wt or WASp-deficient Nalm-6 cells were seeded in the plates at 5×10^4/100 μL. After a 1-h incubation, the number of adherent cells with a spreading morphology was counted in the indicated area under phase-contrast microscopy. At least 750 cells in eight wells were counted blindly, and the proportion of polarized cells calculated as follows:

$$\%\,\text{polarized cells} = (\text{polarized cell number}/\text{total cell number}) \times 100$$

The cells were then washed with PBS, and firmly attached cells were counted with phase-contrast microscopy. Adhesion to fibronectin-coated 96-well flat-bottomed plates (BD Biosciences, Bedford, MA, USA) was assessed by incubating 5×10^4 cells in the plates for 2 h and then inspecting for adherent cells with phase-contrast microscopy. The cells were also stained with Rhodamine-conjugated phalloidin (Sigma, St. Louis, MO, USA) and were inspected under a fluorescence microscope (Zeiss).

Stimulation of Nalm-6 cells for signal transduction assay

Wt or WASp-deficient Nalm-6 cells in Hanks' balanced salt solution (HBSS) at 2×10^6/200 μL were stimulated with 2 μg of anti-CD9 mAb (ALB6) for pre-established times. For stimulation with CD47, the cells were put into anti-CD47 mAb-precoated 24-well plates at 1×10^6/400 μL, incubated at 20°C for 2 min, and then stimulated by incubating the plate at 37°C for pre-established times. The reaction was quenched by adding 600 μL of ice-cold HBSS and subsequently centrifuging the collected cells.

Induction of apoptosis by crosslinking of CD24 and detection of apoptosis by flow cytometry

Wt or WASp-deficient Nalm-6 cells were stimulated with anti-CD24 mAb (5 μg/ml) in the presence of rabbit secondary anti-mouse IgG antibody (10 μg/ml) for indicated time period. To detect apoptosis induced by crosslinking of CD24, the cells were stained with FITC-labeled Annexin V (Roche Applied Science, Mannheim, Germany) and 7-AAD (Sigma, St. Louis, MO, USA). The cells were then analyzed by flow cytometry according to the manufacturer's instruction.

Western blot

The cell lysates were prepared by incubating cells in a lysis buffer [1% NP40, 20 mM Hepes (pH 7.55), 150 mM NaCl, 50 mM NaF, 1 mM Na3VO4] supplemented with protease inhibitor cocktail (Sigma, St. Louis, MO, USA) for 30 min on ice. The lysates were centrifuged at 14,000 rpm at 4°C for 30 min and stored at −80°C until further analysis.

Western blot analysis with anti-phosphotyrosine antibody (4G10), anti-CD43 (L10), or anti-WASp antibody (5A5) was carried out as previously described [4, 44]. Rabbit polyclonal antibody to Btk phosphorylated at Tyr223, Syk phosphorylated Tyr525/526, Src phosphorylated Tyr416, and PLCγ1 phosphorylated at Y783 were sourced from Cell Signaling Technology. Rabbit polyclonal antibody to Lyn phosphorylated at Tyr396 was obtained from Abcam. An equal amount of loading was confirmed by staining the transferred blot with Ponceau S or by probing with anti-β-actin antibody.

Immunoprecipitation

Immunoprecipitation was carried out as previously described [4, 44]. Briefly, the cell lysates were incubated with protein G Sepharose beads (GE Healthcare Life Sciences) preadsorbed with normal rabbit serum/normal mouse serum overnight. The precleared cell lysates were